NASA Contractor Report 174762

Effects of Cobalt, Boron, and Zirconium on the Microstrucutre of Udimet 738

Todd G. Nakanishi

Purdue University
West Lafayette, Indiana

September 1984

Prepared for

NATIONAL AERONAUTICS AND SPACE ADMINISTRATION
Lewis Research Center
Under Contract NAG 3-59

ENTER:

3 1 1 RN/NASA-CR-174762
DISPLAY 03/6/1
85N10166** ISSUE 1 PAGE 27 CATEGORY 26 RPT#: NASA-CR-174762 NAS 1.26:174762 CNT#: NAG3-59 84/09/00 76 PAGES UNCLASSIFIED DOCUMENT
UTTL: Effects of cobalt, boron, and zirconium on the microstructure of Udimet 738 TLSP: M.S. Thesis. Final Report
AUTH: A/NAKANISHI, T. G.
CORP: Purdue Univ., Lafayette, Ind. AVAIL.NTIS SAP: HC A05/MF A01
MAJS: /*ALLOYS/*BORON/*COBALT/*MICROSTRUCTURE/*STRUCTURAL STABILITY/*ZIRCONIUM
MINS: / CHEMICAL ANALYSIS/ ELECTRON MICROSCOPY/ FRACTOGRAPHY/ HEAT TREATMENT/ METALLOGRAPHY/ RUPTURING/ SOLIDIFICATION/ X RAY DIFFRACTION
ABA: R.S.F.

TABLE OF CONTENTS

I. INTRODUCTION

In the United States, superalloy development began during the 1930's prompted by the need for heat resistant materials required in aircraft engine turbosuperchargers. Since then gas turbine engine technology has paced the development of new superalloys. In a gas turbine, the first stage turbine blades or buckets are cast parts which can see longitudinal stresses of approximately 138 MPa and temperatures ranging from 650 to 980^{o}C. Future demands on performance and efficiency will push these limits even higher each year.

In order to achieve these "super" properties, many alloying elements are added to the base element resulting in complex microstructures. The major alloying elements of Ni-base superalloys include; chromium (Cr), cobalt (Co), aluminum (Al), titanium (Ti), tantalum (Ta), niobium (Nb), tungsten (W), and molybdenum (Mo). Carbon (C), boron (B), and zirconium (Zr) are considered as trace or minor element additions.

Cr, Co, Ta, Nb, and W are imported from foreign countries and are considered to be critical or strategic elements. In recent years, the political uncertainty in countries producing these strategic elements has prompted

studies of the roles of strategic elements in superalloys. Large amounts of cobalt are used in superalloys, yet the role of cobalt is not well understood. Cobalt has been found to have various roles in different alloys; however, the main role of cobalt apparently is to modify the the matrix solubility for alloying elements thereby affecting microstructures and mechanical properties.

To understand the role of cobalt and its interactions with boron and zirconium from solidification to long time aged effects, cast U-738 was chosen since it is a high Cr alloy and is being extensively used in gas turbines for oxidation and sulphidation resistance. This study on U-738 will attempt to reveal the effects of Co, B, and Zr on:

1. Solidification behavior.
2. Precipitation of new phases.
3. Overall changes in morphology of existing phases.
4. Structural stability during exposure.
5. Mechanical properties.

Morphologies of γ', primary and secondary carbides, boride formation, eutectic γ', and the grain boundaries will be evaluated and then correlated to mechanical property data. Structural characterization by scanning electron microscopy, energy dispersive X-ray analysis (EDAX), and X-ray diffraction of extracted phases will be carried out.

II. LITERATURE REVIEW

2.1 Phases Found in Superalloys

Nickel base superalloys consist of a variety of elements. There may be as many as ten to twelve major elements and an equal number of trace elements. Nickel and cobalt are face centered cubic elements which prefer the austenite gamma matrix (γ). Solid solutioning elements include iron, chromium, molybdenum, tungsten, and vanadium. Elements which may partition to form the coherent precipitate γ' (Ni_3Al) include aluminum, titanium, columbium, and tantalum. Boron, carbon, zirconium, and hafnium are trace elements which form borides and carbides, and segregate to the grain boundaries.[1] Generally all these elements combine to form five distinct phases, the matrix, gamma prime (γ'), carbides, borides, and TCP (tetragonally close packed) phases.

Gamma prime is a unique precipitate that is inherently ductile and contributes to alloy strength by dislocation interaction, and antiphase boundary strengthening. The strength of γ' increases with temperature[1]. Gamma prime nucleates homogeneously due to its compatible FCC structure and lattice constant (0.1% mismatch). As a result it has low surface energy and extraordinary long time stability[1].

Carbides may form in a various number of ways. Upon solidification MC type carbides form heterogeneously

throughout an alloy and may be found intergranularly or transgranularly (often interdendritically)[1]. Chemically these primary carbides contain titanium, tantalum, niobium, and hafnium. They have a FCC structure and will decompose during heat treatment to provide carbon for secondary carbide reactions. The secondary carbide reaction is usually the very important Cr rich $M_{23}C_6$ type carbide which forms in the range from 760 to 980°C. Molybdenum and tungsten as well as nickel can be found in the $M_{23}C_6$. $M_{23}C_6$ carbides generally form in the grain boundaries, significantly improving rupture strength[1] by preventing grain boundary sliding. However rupture failure often initiates either by brittle fracture of these same carbides or through decohesion of the $M_{23}C_6$ - γ interface.

M_6C carbides, typically $(Ni,Co)_3(Mo)_3$ or $(Ni,Co)_2(W)_4$, may form if the Mo plus W is greater or equal to 7 wt%. Often they will form in the matrix as either discrete particles or plates within a temperature range of 815 to 980°C.

Discrete MC, $M_{23}C_6$, and M_6C carbides have been shown to have beneficial effects on mechanical properties by dispersion strengthening and controlling grain growth. When they form plates, needles, or continuous films in grain boundaries, the mechanical properties can be impaired.

Borides may form upon solidification or as a result of heat treatment. The M_3B_2 boride is the most common type

found. Boride formation may occur when boron is in excess of .012 wt%[1] in nickel-base alloys. However, borides may be found in Ni-base alloys with less than 120 ppm of boron due to segregation. Boron generally segregates at the grain boundaries, and can be part of the $M_{23}C_6$ carbide.

Laves, σ, and mu are hard TCP phases which form upon heat treatment. TCP phases are platelike in nature and can nucleate at grain boundaries and in the matrix. The plate-like morphology of these phases provides excellent nucleation sites for crack initiation and propagation leading to low temperature brittle failure.[1]

2.2 Physical Metallurgy of U-738

A study by Betner et al .[2] described the phases found in the alloy IN-738. After the standard heat treatment two sizes of γ′ were observed, one about 0.1 micron and the other about 1.5 to 2.5 microns. The finer γ′ was more rounded and the coarser more angular. Solutioning of the as cast γ′ in alloy 738 began at 980°C and was not complete until an hours exposure at 1204°C. 500 hours exposure at 820°C showed a disappearance of the fine secondary γ′.

MC carbides were found dispersed interdendritically and in the grain boundaries and had a lattice parameter of 4.36Å. After 2000 hours at 820°C much of the MC carbides were still present along with a nearby rod-like phase.

$M_{23}C_6$ carbides were found primarily intergranularly and formed as a function of temperature at the expense of the MC phase. The solution temperature of $M_{23}C_6$ was found to be 1037°C. Many N_v calculations were made to estimate σ formation tendency and it was concluded that alloy 738 is stable; however, a slight variation in composition could strongly promote σ phase.

2.3 Effects of Cobalt

The role of cobalt in superalloys has been an area of great interest in recent years. Several papers have revealed the effect of cobalt on γ′, carbide formation, alloy stability, and mechanical properties in nickel-base superalloys.[3-10] Cobalt has a varying role depending on the overall composition of the alloy.

In a study by Engel, it was observed that removal of cobalt in Udimet 700 resulted in an increased amount of unsolutioned primary γ′ and a decrease in amount of fine secondary γ′.[3] Jarret and Tien also noted a decrease in fine γ′ due to less solutioning.[6] A study of the alloy Mar-M247 by Nathal et al. revealed that upon removal of cobalt, the γ′ solvus temperature was raised by 30°C.[4] However, Mauer et al. found that in Waspaloy, the γ′ solvus was unaffected by the removal of cobalt.[9]

Cobalt has also been found to effect the weight percent of γ' in Ni-base alloys. Heslop claimed that cobalt increased the amount of γ' found in Nimonic superalloys. He stated that the mechanism was a decreased matrix solubility for Al and Ti thereby increasing the γ' precipitation.(7) Studies by Mauer et al. and Nathal et al. reported a decrease in the wt% of γ' in when cobalt was reduced.(9,4) This agrees with the results found by Heslop. Engel noted that the weight fraction of γ' in U-700 was unaffected by removal of cobalt.(3) Nathal et al. also observed a reduction in area fraction of eutectic γ' islands and an increase in secondary γ' size upon removal of cobalt.(4) Jarret and Tien claimed that the γ' coarsened more readily in their cobalt free alloy due to no $M_{23}C_6$ pinning of the primary γ'.(6)

Cobalt also significantly influences the formation of carbides. In his fundamental study, Heslop concluded that cobalt increased the solubility of the matrix for carbon, thus inhibiting the formation of grain boundary $M_{23}C_6$ carbides.(7) Mauer et al. found that removal of cobalt in Waspaloy resulted in increased precipitation of both MC and $M_{23}C_6$ carbides.(9) Engel noted that cobalt removal promoted $M_{23}C_6$ formation; however, M_3B_2 precipitation increased as cobalt was added.(3) Upon long time aging (LTA), Nathal et al. reported that additional $M_{23}C_6$ carbides and continuous carbide films formed in the grain boundaries upon remo-

val of cobalt.[4] Jarret and Tien noted a slightly different carbide alteration when cobalt was removed from Udimet 700. They found that removal of cobalt, especially down to 0 wt%, produced $M_{23}C_6$ and MC carbides upon solidification. These $M_{23}C_6$ carbides more likely formed upon slow cooling after solidification thereby appearing in the "as cast" microstructure. They also found that upon aging, the 0 wt% cobalt alloy displayed little additional grain boundary precipitation of $M_{23}C_6$ and attributed it to the relatively stable "as cast" $M_{23}C_6$.[6] With regard to σ phase stability, Lund et al. performed a detailed study on the role of cobalt in σ formation. They noted that cobalt in small amounts inhibited σ phase formation and at around 5 wt%, cobalt increased the γ' precipitation, displacing Cr from the matrix thereby making it available for formation of σ. Engel, Jarret, and Tien reported that cobalt in excess of approximately 8 wt% promoted σ phase.[3,6]

Cobalt also has an impact on mechanical properties of nickel-base superalloys. While this may in part be due to its solid solution effects, primarily it is due to its influence on microstructure. Tensile properties are apparently least affected. Nathal et al. , Jarret and Tien, and Mauer et al. all reported little change in tensile strength and ductility when cobalt was removed from their respective alloys.[5,6,9]

Creep/stress rupture properties were most influenced. Nathal et al. and Mauer et al. found that cobalt increased the stress rupture life of Mar-M247 and Waspaloy respectively by three fold.[5,9] They also stated that removal of cobalt increased the creep rate up to six fold, yet the ductility in these tests were uninfluenced. Jarret and Tien investigated alloys with various heat treatments.[6] They found that in U-700, stress rupture life was significantly lowered when alloys with less than 8.0 wt% Co were given a disk heat treatment (partial γ' solutioning). However, in the same alloys which were given a blading heat treatment (fully solutioned γ'), the stress rupture life was virtually unaffected.

2.4 Effects of Boron and Zirconium

Boron and zirconium are added to nickel-base superalloys in small amounts and are therefore referred to as trace elements. In the late 1950's it was realized that trace amounts of these elements markedly improved hot working behavior and creep rupture properties of these alloys.[12] How B and Zr improve mechanical properties is not clearly understood yet they are considered "essential" elements.[1]

A study by Antony and Radavich extensively studied the microstructural results of Zr and B additions and their effect on stress rupture properties.[11] They found that Zr

additions of .15 wt% increased the solidification range of their alloy by 16°C resulting in more microporosity which reduced 760°C stress rupture life drastically. However, the 928°C stress rupture life improved and was attributed to zirconiums effect on MC morphology. Zr was found to alter the existing script Ta,Ti MC carbides to a Ta rich discrete MC phase. In addition, Zr suppressed the formation of a grain boundary film. This film formed at high B levels and lower Zr levels.

Zr was found to promote larger and more numerous eutectic γ' islands, around which a Zr rich "stick" phase could be seen. At the highest levels of Zr, the stick phase also appeared in the grain boundaries. Boron, contrary to the binary Ni-B phase diagram, actually decreased the solidification range. Less microporosity formed and a large increase in stress rupture life at both 760 and 928°C occurred.

Boron was also found to effect grain boundary precipitation. With no B, fine MC precipitates formed in the grain boundaries whereas at high B levels the grain boundary contained primarily the $M_3 B_2$ phase. Borides also formed in a script like fashion near the eutectic γ' islands when added at .012 wt%. However, they changed to massive type precipitates at .025 wt%. Antony and Radavich also concluded that the boride phase precipitated directly from the liquid phase during the latter stages of solidification.

Decker and Freeman studied the possible mechanisms that result in the beneficial effects of B and Zr.[13] They found that low B and low Zr content (approximately 0 wt%) resulted in rapid agglomeration of $M_{23}C_6$ and γ' in the grain boundaries, followed by depletion of γ' and intergranular cracking transverse to the applied stress. Microcracking initiated between $M_{23}C_6$ particles and the depleted zones. Additions of Zr, B, and Zr plus B in that order retarded this process thereby increasing rupture life. Their conclusion was that Zr and B stabilized the grain boundary by inhibiting excessive $M_{23}C_6$ formation. They also concluded that B promoted the formation of carbides within the matrix.

A summary of most of the work which has been performed with regard to B and Zr in superalloys was written by Holt and Wallace.[12] They state several examples of how these elements have been shown to increase rupture life 13 times, elongation 7 times, high temperature strength, ductility, and notch sensitivity. Holt and Wallace presented many suggestions that B and Zr are involved in interaction with interstitials and impurity elements. For example, Zr is known to interact with sulphur and carbon as a scavenger forming sulphocarbides. This lowers the amounts of these elements remaining in solid solution at the grain boundaries. Although there is no evidence that boron combines with sulphur, it has been suggested that boron alters sulphide morphology from plate like to spheroidal and that its

solidus depressing effect may aid in the gettering of sulphur and other detrimental impurities. It has also been suggested that boron reduces secondary grain boundary precipitation by shunting carbon to the matrix.

It is generally agreed that B and Zr segregate to the grain boundaries due to their odd atomic size and low solubilities in γ and γ'. Boron is much smaller in atomic size than Ni and tends to locate interstitially while Zr is large in atomic size compared to Ni. In the grain boundaries they are believed to fill vacancies, reducing the formation of γ' denuded zones. In addition it has been suggested that they both be present during solidification to prevent oxygen and sulphur from forming continuous films in the grain boundaries.

A study by Hu and Li revealed that B initially segregated to the grain boundary, the carbide-matrix interface, and in the borocarbide $M_{23}(C,B)_6$.[14] After aging they discovered that the boron then segregated to the MC carbide periphery resulting in MC degeneration into more $M_{23}(C,B)_6$.

Studies by Woodford and Bricknell have considered environmental damage to nickel-base superalloys and how it is regulated. In a study by Woodford, oxygen was determined as the detrimental species.[15] Oxygen segregation can lead to grain boundary immobilization and unstable intergranular fracture. He found that B additions reduced this suscepti-

bility. In a later paper Woodford and Bricknell showed that B was effective in preventing preferential grain boundary precipitation of complex oxides during air exposure.[16]

Floreen and Davidson concluded that B and Zr improved the creep properties in a nickel-base superalloy.[17] Although their primary effect appeared to be minimization of the harmful effects of oxygen, they also state that no single mechanism can explain all observed effects and their efficacy may vary with alloy composition and test conditions. They also noted no changes in microstructure, fracture appearance, or grain boundary sliding behavior due to B and Zr additions.

Zr at a level of 1 wt% in a Ni-Cr-Zr alloy, was found to be beneficial in preventing environmental attack.[18] The mechanism was described as a rapid and more extensive nucleation of Cr_2O_3 along the alloy surface. A similar result occurred in a H_2,H_2S atmosphere.

In a study on Zr effects in alloy 713C, Radavich found zirconiums influence primarily to be changes in γ' and MC carbides.[19] Alloy 713C with low Zr showed no eutectic islands and ragged primary γ'. Increasing Zr resulted in more regular primary γ' and large quantities of eutectic islands. Alloy 713C with low Zr also displayed chinese script MC carbides in the grain boundaries. Increasing the Zr in 713C created a more blocky, discrete, and higher

parameter MC. It was also noted that σ was found near eutectic islands and grain boundaries, although Zr showed little influence on its formation. Overall the grain boundary precipitates displayed a decrease in quantity with increased Zr levels.

III. EXPERIMENTAL PROCEDURE

3.1 Materials

Twelve experimental heats of Udimet 738 were prepared by the Special Metals Corporation (SMC), a division of Allegheny Ludlum Industries in New Hartford, New York. The heats varied compositionally by systematically replacing cobalt, boron, and zirconium with nickel. The alloy classification and corresponding weight percent (wt%) of the variable elements are given in Table I. The remaining elements of each alloy were held constant. The industrial standard composition for Udimet 738 is alloy 1A.

Each heat was investment cast in "cast to size" test bars with a test region diameter of .635 centimeters. These test bars provided samples for microstructural analysis as well as mechanical testing.

3.2 Heat Treatment of Cast U-738

Cast bars of U-738 were given the commercial standard heat treatment of 1121^{o}C for 2 hours in vacuum, back cool with an inert gas (Ar or N) to room temperature.

TABLE I. Alloy Compositional Variation (wt%)

Alloy No.	Cobalt	Boron	Zirconium
1A	8.5	.01	.04
1B	8.5	.03	.04
2A	8.5	.01	.10
2B	8.5	.03	.10
3A	8.5	.01	.20
3B	8.5	.03	.20
4A	0.0	.01	.04
4B	0.0	.03	.04
5A	0.0	.01	.10
5B	0.0	.03	.10
6A	0.0	.01	.20
6B	0.0	.03	.20

Remaining composition of all alloys (wt%)

Al	Ti	Ta	Nb	W	Mo	Cr	C	Ni
3.4	3.4	1.7	0.9	2.6	1.7	16.0	0.1	Bal.

The samples were aged at 843°C for 24 hours and air cooled to room temperature.

3.3 Structural Stability

Alloy stability was evaluated by exposing the as cast and the solution treated samples at 843°C up to 500 hours. The effects of the variations in cobalt, boron, and zirconium on the tendency for sigma formation would manifest themselves at this temperature.

3.4 Mechanical Testing

Specific mechanical properties of all twelve alloys were obtained to evaluate any effects that the compositional modifications may induce. The two tests chosen were uniaxial room temperature tensile, and uniaxial elevated temperature stress rupture. Commercial specifications are given in Table II. The samples tested were each heat treated to the industry standard.

All testing was performed at the Gas Turbine Division of General Motors Corporation, Indianapolis Indiana. Standard testing procedures were followed and the data sheets appear in Appendix B. Tested samples provided fracture surfaces for fractographic examination.

3.5 Sample Preparation And Examination

All samples were prepared by wet polishing through 600 grit silicon carbide. This was followed by an electropolish in 20% sulphuric acid in methanol and an immersion etch in 15% hydrochloric acid in methanol plus a few drops of hydrogen peroxide.

Optical and scanning electron microscope (SEM) observation of these prepared samples provided microstructural characterization data. During SEM observation, energy dispersive analysis of X-rays (EDAX) provided qualitative

chemical analysis of phases *in situ*. These phases were then extracted for X-ray diffraction identification. Details of these techniques are located in Appendix A.

TABLE II. Mechanical Property Specifications

Room Temperature Tensile Properties			
S_u (MPa)	S_y (MPa)	%Elongation	%Reduction of Area
896.3	792.9	3.0	3.0

Stress Rupture Properties at 982°C and 151.8 MPa	
Life (Hrs)	%Elongation
30	5.0

IV. RESULTS

The results of this study are grouped into three categories; scanning electron microscopy, mechanical properties, and phase extraction identification. The first category discusses the microstructural characteristics as a function of compositional variations and heat treatment relative to the standard alloy 1A. Mechanical property data is presented and related to compositional changes, microstructural differences and fractograghic observations. Finally, identification of extracted residues is presented.

4.1 Scanning Electron Microscopy

4.1.1 Standard Alloy Composition - 1A

The standard composition of U-738 contains 8.5 wt% Co, .01 wt% B and Figure 1 shows representative microstructure in the as cast, as cast plus solutioned, and "aged" conditions of the commercial standard composition of U-738. In the initial as cast condition, large script titanium rich MC carbides can be found throughout the sample. They occupy grain boundary and interdendritic locations. Two sizes of cooling or as cast γ' were found which indicate areas of compositional variation. The as cast γ' generally appears starlike and coarse. Moderate sized kidney shaped islands of eutectic γ' were found along grain boundaries and

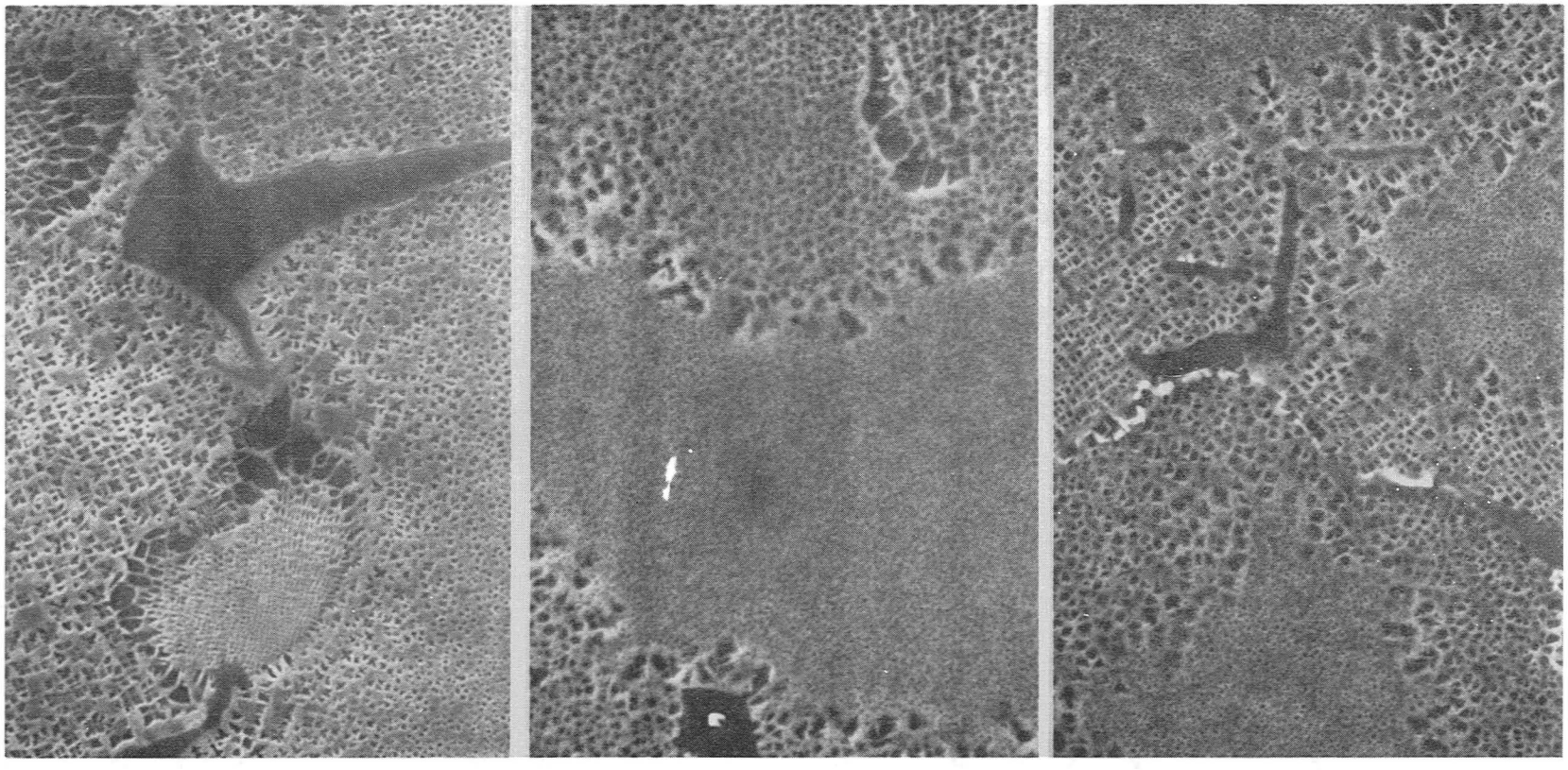

Figure 1. SEM Micrographs of Alloy 1A. (a) as cast 3000X (b) solution treated 2000X (c) aged 24Hrs. 2000X

transgranularly.

Eutectic areas are the last liquid to freeze and therefore contain many odd sized elements resulting in areas of segregation. This provides excellent sites for nucleation of carbides, borides, zirconium rich phases, and deleterious TCP phases. The only precipitates in the as cast eutectic islands and grain boundaries of alloy 1A were script MC carbides.

In the as cast plus solution treated condition, the most visible change in microstructure was the formation of a duplex γ' structure. Because the solutioning temperature of $1121^{o}C$ is in the middle of the γ' solutioning range, only a partial solutioning of γ' takes place. The result is a duplex structure of ultra fine secondary γ' and coarse as cast γ'. The solutioned treated as cast γ' shows a more uniform cuboidal appearance than that in the as cast condition while the eutectic γ' islands exhibit partial homogenization. The MC carbides remained unchanged.

In the solution treated plus aged thermal condition, the precipitation of a Cr rich phase, most likely $M_{23}C_6$ carbides, can be seen along all grain boundaries while a heavier precipitation was noted in the eutectic areas. Very minor breakdown of the primary MC carbides occurred. Overall the as cast γ' appeared more uniform and cuboidal.

4.1.2 Removal of Cobalt - Alloy 4A

Removal of all cobalt while maintaining levels of .01 wt% B and .04 wt% Zr produced various microstructural alterations to alloy 1A. Figure 2 illustrates the three thermal conditions of the cobalt free alloy.

The as cast MC carbides and grain boundaries were very similar to those of alloy 1A. An occasional low melting phase and boride which were not detected in alloy 1A, were found near eutectic γ' areas.

The as cast plus solution treated condition of alloy 4A showed no duplex γ' structure as was seen in alloy 1A. The eutectic islands also exhibited less homogenization. Occasional grain boundary precipitates could be seen in addition to the MC carbides. Because of the Co free nature of this alloy, it is highly probable that these are $M_{23}C_6$ carbides formed upon cooling due to change in carbon solubility.

In the aged condition, much heavier, almost continuous grain boundary precipitates, most likely $M_{23}C_6$, can be seen. This apparent $M_{23}C_6$ precipitation appears heaviest in the eutectic areas. It is possible that some of these precipitates are borides. Breakdown of MC carbides was also more prevalent than in alloy 1A.

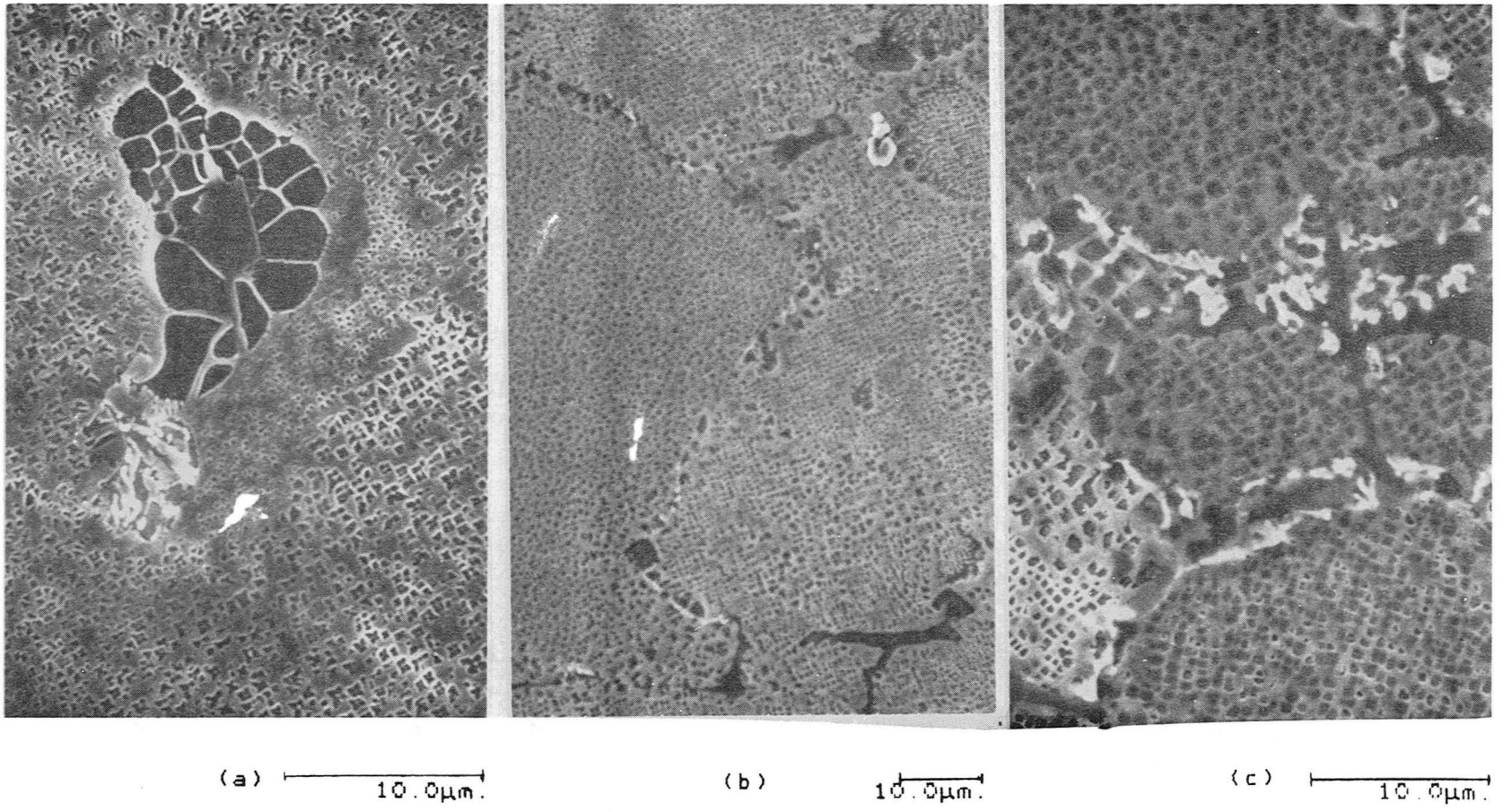

Figure 2. SEM Micrographs of Alloy 4A. (a) as cast 3000X (b) solution treated 1200X (c) aged 24Hrs. 2700X

4.1.3 Addition of Boron - Alloy 1B

Increasing the level of boron in alloy 1A resulted in an alloy with The as cast condition showed precipitation of a Cr, Mo, W rich phase in the eutectic areas. (see Figure 3). This phase appeared blocky and discrete but also appeared script like on occasion and is probably a boride. The eutectic areas were much larger and more numerous than in the base alloy 1A. Some blocky MC carbides were found near the boride precipitates.

After solution treatment, more precipitation of the boride phase occurred in the eutectic areas. A duplex γ' structure resulted upon solution treatment, similar to alloy 1A. Homogenization of the eutectic islands did not occur as completely as in alloy 1A.

After aging, a discrete precipitation of grain boundary $M_{23}C_6$ phase occurred and minor MC breakdown was detected. The as cast γ' showed an increased uniformity in shape and distribution with thermal aging as seen in alloy 1A.

4.1.4 Removal of Cobalt and Addition of Boron - Alloy 4B

Alloy 4B (0 wt% Co, .03 wt% B, .04 wt% Zr) in the as cast condition showed a Cr rich boride phase which was notably larger, more massive, and blocky than in alloy 1B (Figure 4). MC carbides occasionally appeared more blocky than

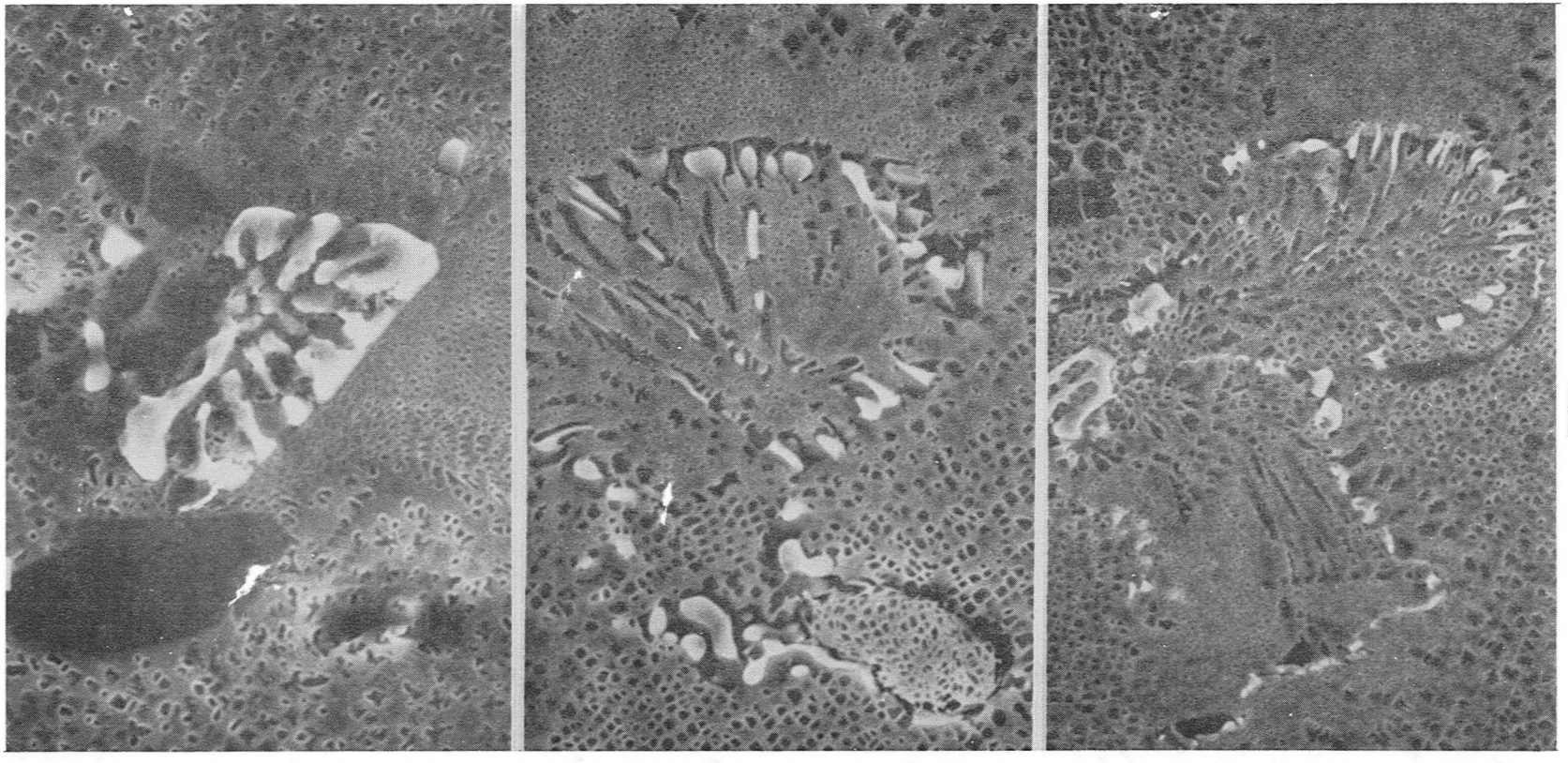

Figure 3. SEM Micrographs of Alloy 1B. (a) as cast 5000X (b) solution treated 3000X (c) aged 24Hrs. 2200X

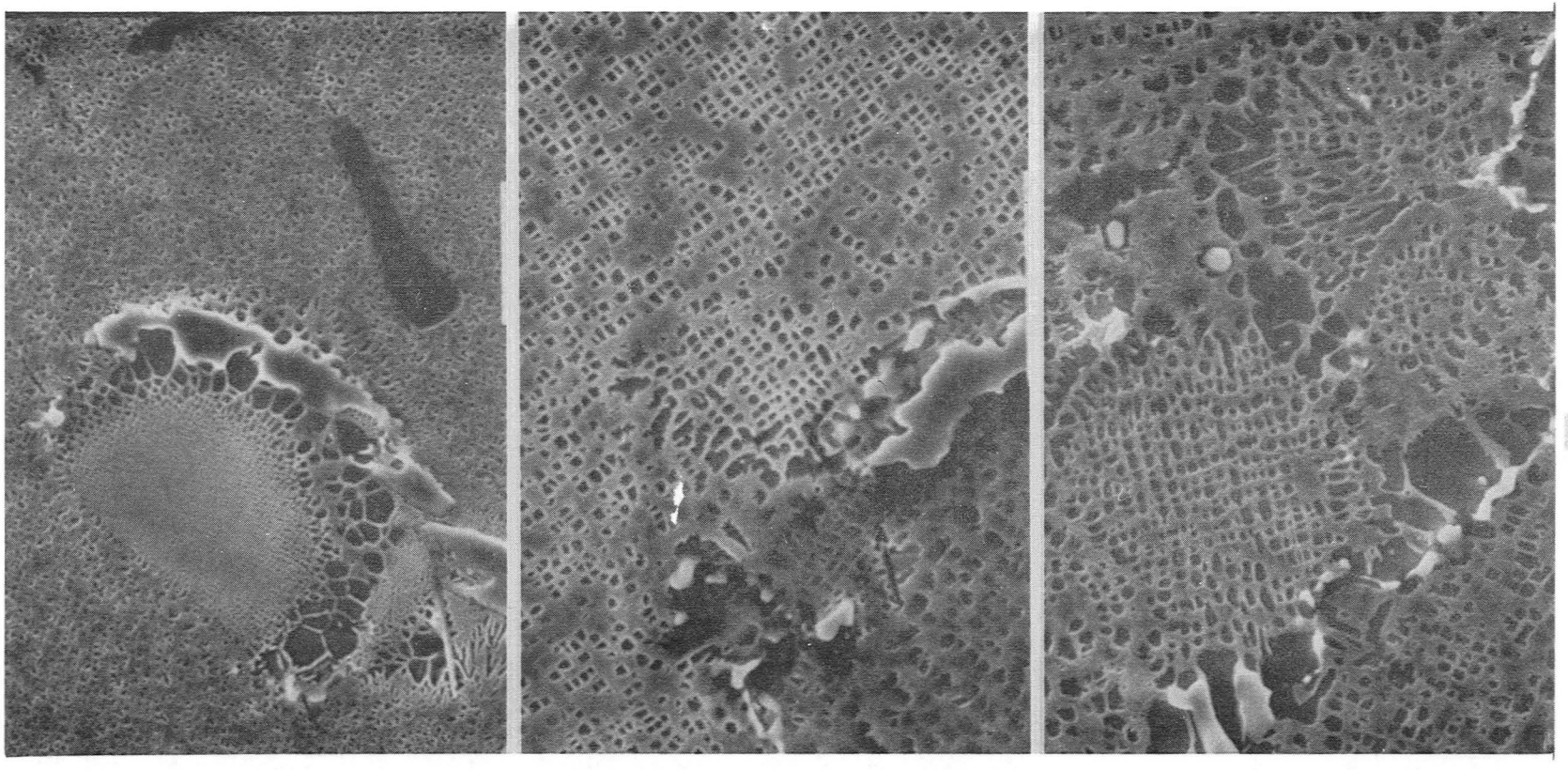

Figure 4. SEM Micrographs of Alloy 4B. (a) as cast 2000X (b) solution treated 3000X (c) aged 24Hrs. 3000X

script type; however, the majority of MC carbides remained script type and were located in grain boundaries or interdendritically as in 1B. The grain boundaries and eutectic γ' islands appeared similar to those in alloy 1B.

Upon solution treatment no duplex γ' structure developed. The eutectic γ' islands showed some homogenization and the as cast γ' became more uniform and cuboidal. These results are similar to those found in alloy 1B. Additional precipitation in the eutectic island periphery suggests more boride formation. Due to decreased carbon solubility resulting from the removal of Co, some of these precipitates may be $M_{23}C_6$ carbides.

After aging, the addition of B seemed to promote fewer discrete $M_{23}C_6$ precipitates in the grain boundaries. Minor MC carbide breakdown was noted and traces of an ultrafine background γ' were observed amidst the as cast γ'. The eutectic γ' islands remained unchanged from the solution treated condition.

4.1.5 Addition of Zirconium - Alloy 3A

Zirconium was varied to three levels; .04 wt%, .10 wt%, and .20 wt%. Because the alloys with .10 wt% level of zirconium showed no substantial microstructural difference relative to the .20 wt% level, the .20 wt% zirconium alloy (3A) was used for evaluation (Figure 5). This alloy

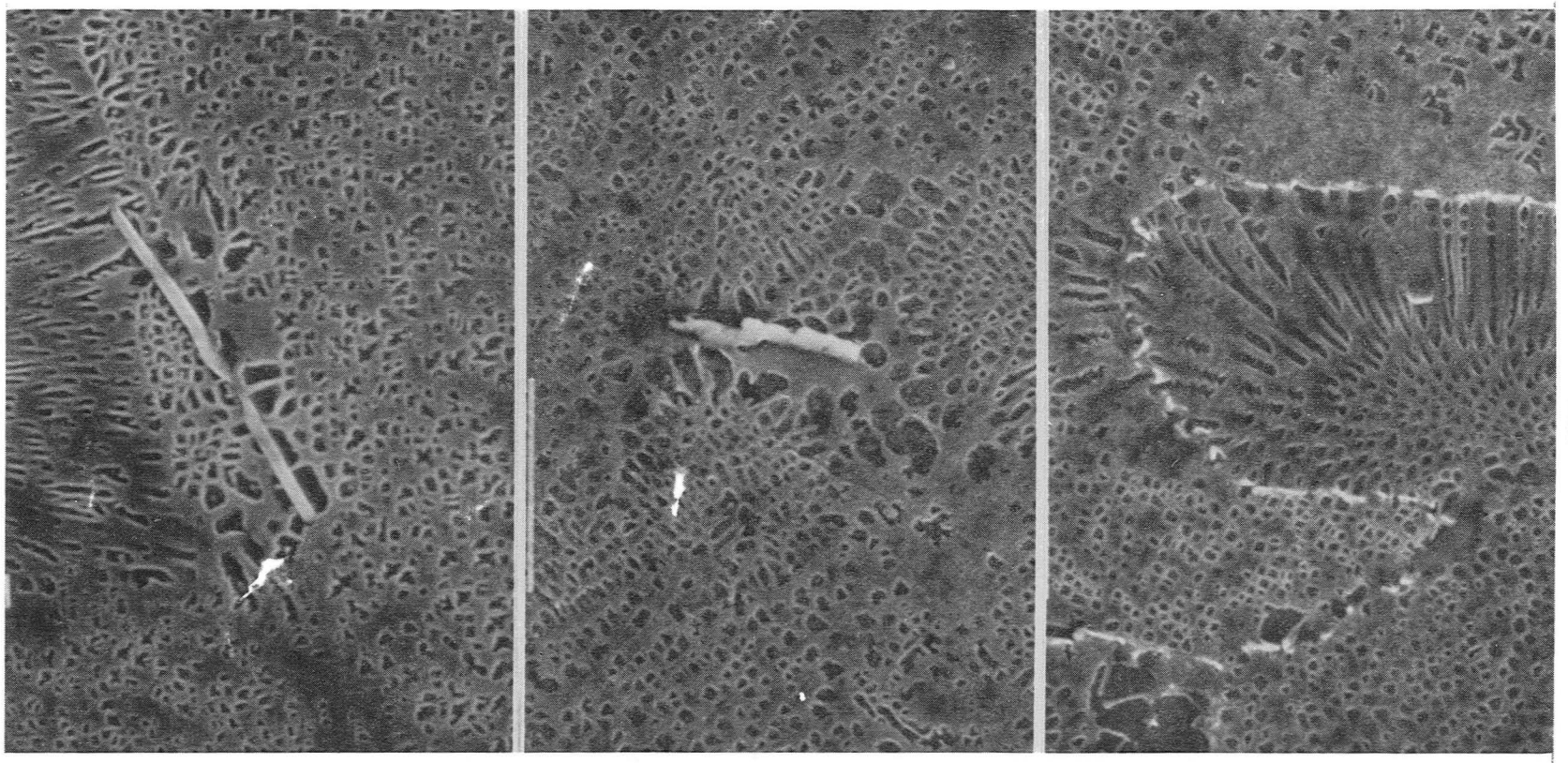

Figure 5. SEM Micrographs of Alloy 3A. (a) as cast 5000X (b) solution treated 3000X (c) aged 24Hrs. 3000X

contained 8.5 wt% Co and .01 wt% B.

The as cast structures of alloy 3A showed two main structural differences relative to the standard alloy 1A. First, the eutectic γ' islands were larger and more numerous. Second, a zirconium rich stick phase precipitated near the eutectic γ' islands. The script MC carbides and grain boundary precipitation appear unaffected by the higher addition of Zr. Overall the as cast γ' appeared slightly more uniform in this higher Zr level alloy as compared to alloy 1A which had the lowest level of Zr.

The solutioning heat treatment produced several structural effects. The eutectic γ' areas showed occasional boride type precipitates even though the level of boron was only .01 wt%. These eutectic γ' areas did not homogenize as completely as the low Zr alloy 1A. Occasionally a low melting phase was observed in these same locations. The Zr rich stick phase remained unaltered in location, size, and shape. The as cast γ' in alloy 3A exhibited solutioning but to a lesser degree compared to alloy 1A.

The aging treatment produced discrete grain boundary precipitation of $M_{23}C_6$ carbides. Some Zr sticks were also found in the grain boundary and the MC breakdown was very minor. The remaining structures apeared similar to those in the solutioned condition.

4.1.6 Removal of Cobalt and Addition of Zr - Alloy 6A

Alloy 6A contains 0 wt% Co, .20 wt% Zr, and .01 wt% B. This cobalt free alloy showed minor variations in as cast phases compared to alloy 3A (Figure 6). Occasional boride type precipitates on the eutectic island periphery and more numerous ultra fine γ' precipitating between the coarse as cast γ' appear in the as cast structure of alloy 6A. These structures do not appear in alloy 3A.

The solutioning heat treatment did not produce as distinct a duplex γ' structure as seen in other cobalt free alloys. The eutectic γ' areas displayed less homogenization than in alloy 3A.

The aging heat treatment resulted in slightly heavier $M_{23}C_6$ precipitation in the grain boundaries than in alloy 3A. Alloy 6A, having the highest level of Zr, appeared to have less continuous precipitation of $M_{23}C_6$ in the grain boundaries than alloys of lower Zr levels and 0 wt% Co. Fairly heavy breakdown of MC carbides was also noted in alloy 6A. The ultrafine γ' and partially homogenized eutectic γ' remained unchanged relative to these same structures in the solutioned condition.

4.1.7 Additions of Boron and Zirconium - Alloy 3B

The microstructures of alloy 3B are shown in Figure 7.

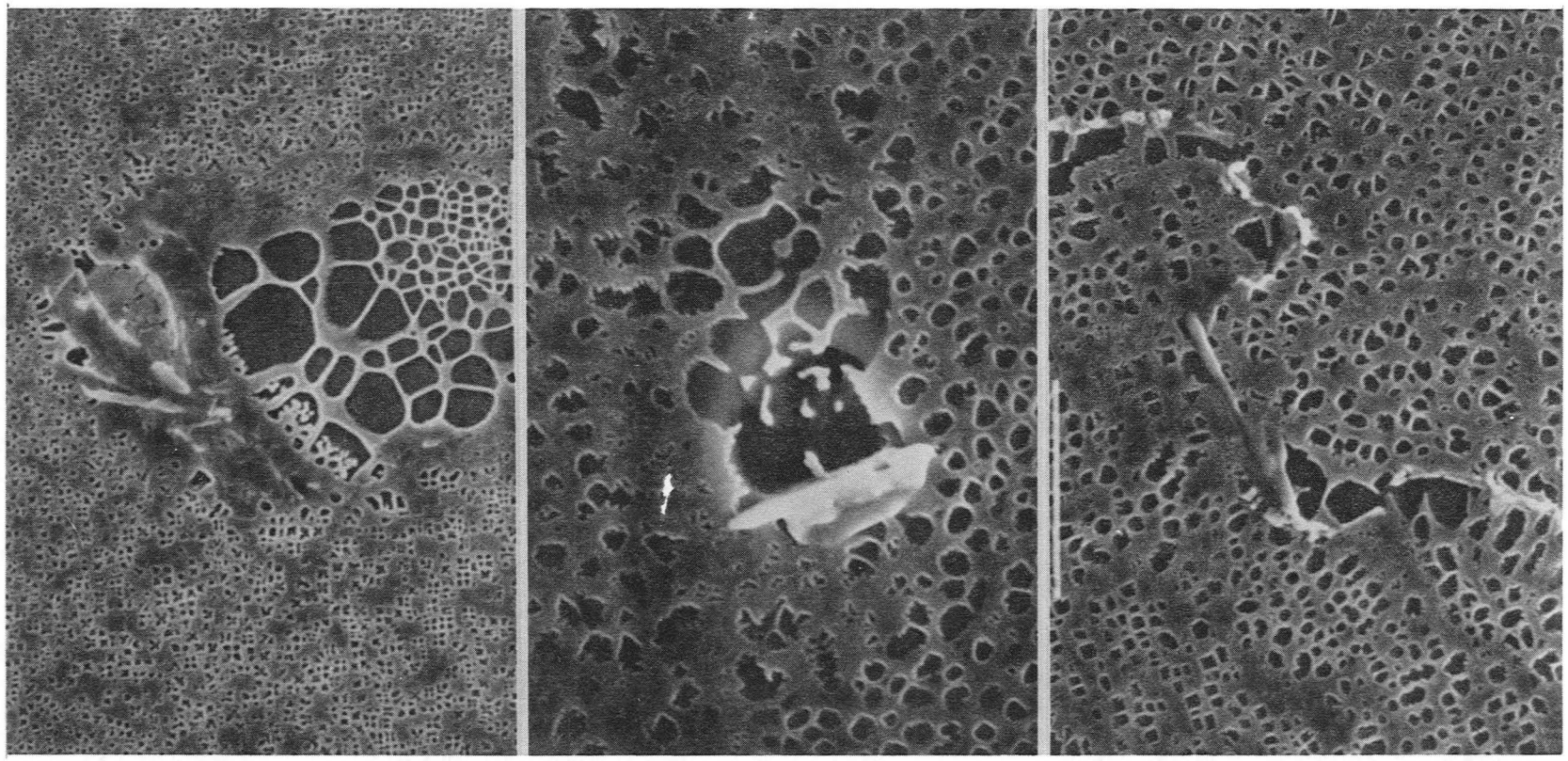

Figure 6. SEM Micrographs of Alloy 6A. (a) as cast 3000X (b) solution treated 5000X (c) aged 24Hrs. 3000X

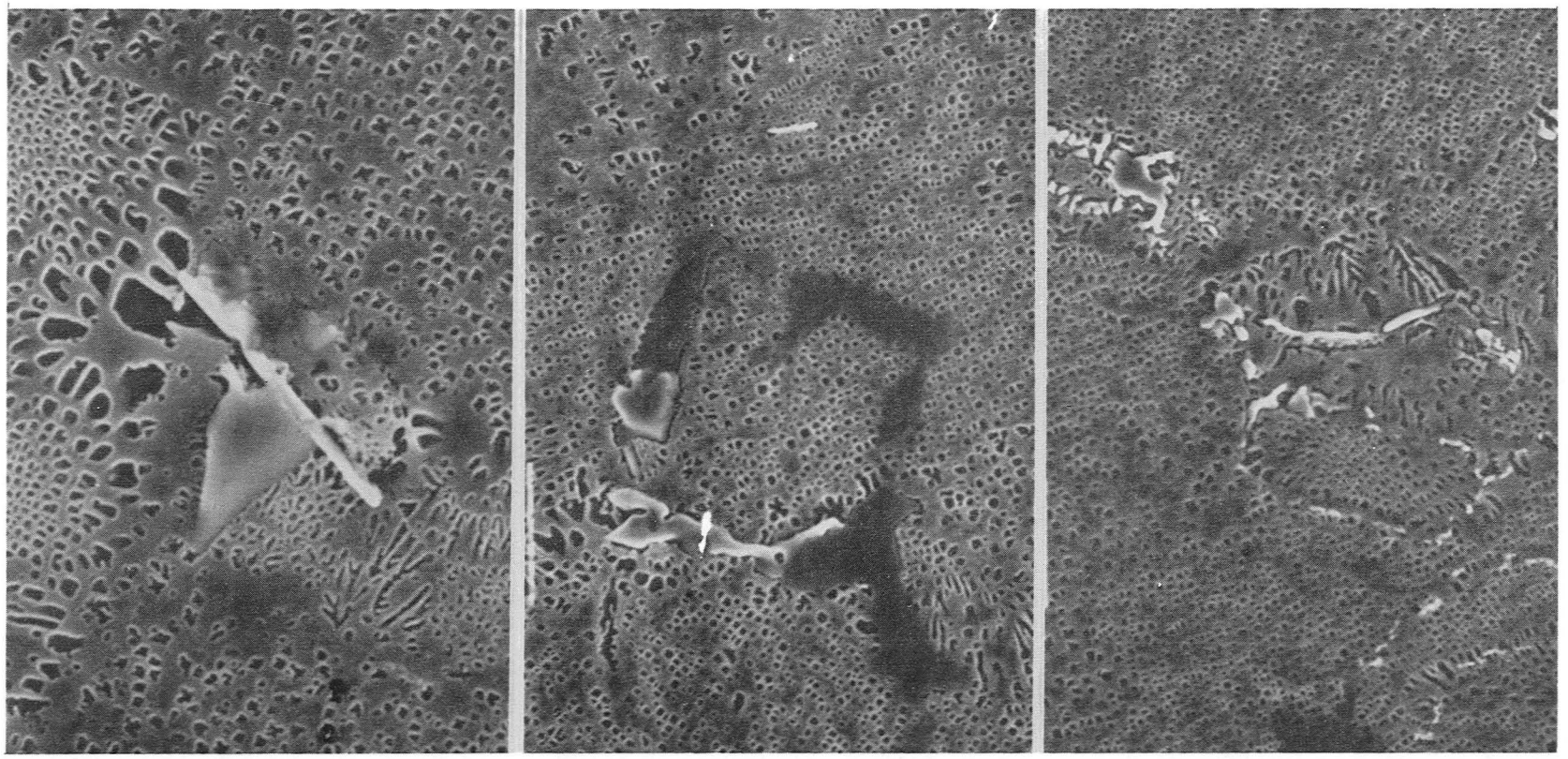

Figure 7. SEM Micrographs of Alloy 3B. (a) as cast 5000X (b) solution treated 2000X (c) aged 24Hrs. 1800X

Alloy (3B) contains .03 wt% B, .20 wt% Zr, and 8.5 wt% Co. Compared to alloy 1A, the as cast MC carbides and the grain boundaries appear unaltered by the high B and Zr content found in alloy 3B. However, more frequent borides and larger, more numerous eutectic γ' were found in alloy 3B than in the alloys with a low level of Zr (1B). Occasionally a Zr rich stick and a boride were observed together as in Figure 7. The borides were more blocky, fairly discrete, and found in the eutectic γ' areas.

After the solutioning heat treatment, the borides appeared to coarsen resulting in some massive boride particles. The MC phase appeared to be stable and the grain boundaries showed no signs of precipitation. The eutectic areas showed less signs of homogenization than those in alloys with less Zr and less B. A less distinctive duplex γ' structure was observed in alloy 3B; therefore, the solutioning of the as cast γ' was not as extensive as in alloys with less Zr.

After the aging heat treatment, discrete $M_{23}C_6$ carbides were observed in the grain boundaries along with minor MC breakdown. This observation was made in all alloys which contained Co. Fine secondary γ', Zr rich sticks, and boride phases remained unchanged from the solution treated condition. Coarse as cast γ' appeared more cuboidal and the eutectic γ' islands showed no additional homogenization.

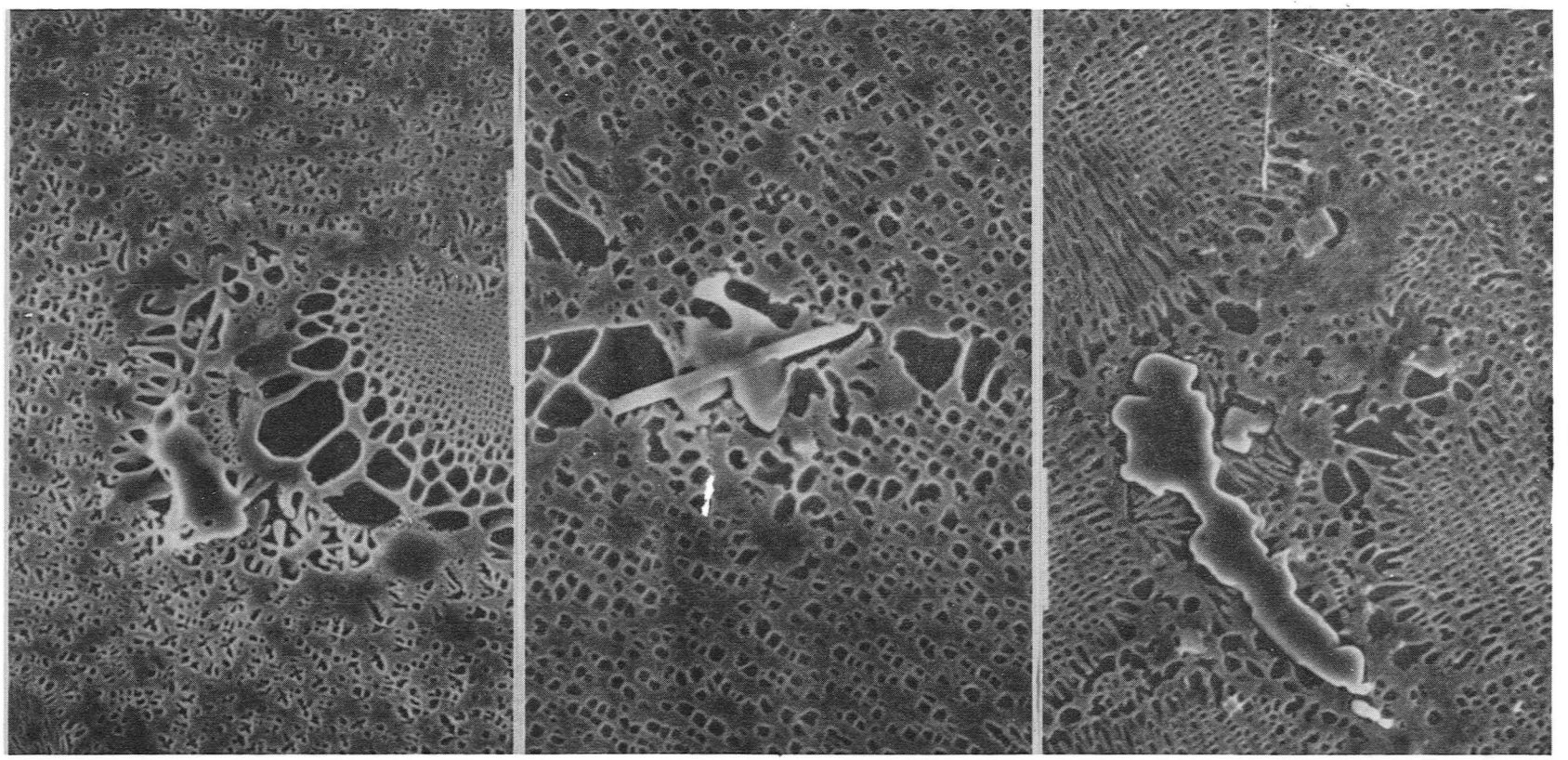

Figure 8. SEM Micrographs of Alloy 6B. (a) as cast 3000X (b) solution treated 3000X (c) aged 24Hrs. 2000X

4.1.8 Alloy 6B - 0.0% Co Plus Additions of B and Zr

As cast alloy 6B with 0 wt% Co, .03 wt% B, and .20 wt% Zr is shown in Figure 8. Borides, MC carbides, grain boundaries, and eutectic γ' areas were similar to those observed in the cobalt containing alloy 3B. The only difference appeared to be a few additional Zr rich sticks.

After the solutioning treatment, no duplex γ' structures were noted, and an ultrafine background γ' appeared slightly more numerous than in alloys with lower boron and zirconium levels. The eutectic areas remained large and appeared unaffected by the heat treatment. Other structures were essentially unchanged from those in the as cast condition.

Aging produced two noticeable structural changes. First, a fairly discrete and infrequent precipitation of $M_{23}C_6$ in the grain boundaries and second a plate phase precipitate in the matrix were found. The plate phase was high in Cr and may be the TCP phase sigma (σ). These plates occurred infrequently and also appeared in the cobalt free alloys 5A and 5B.

4.1.9 Alloy Stability

Structural stability of all twelve alloys was determined by aging at 843°C. At this temperature, σ formation and/or heavy $M_{23}C_6$ precipitation occurs if the alloys are compositionally unstable. Both as cast alloys and solution treated alloys were aged for 100, 300, and 500 hours.

Overall, less plate formation was found in the as cast alloys even though normally as cast alloys show more segregation. Trends of instability were otherwise similar in both as cast and solution treated alloys. They were as follows:

1. High levels of boron (.03 wt%) apparently promoted plate phase formation in as little as 100 hours of aging.

2. Removal of cobalt accelerated plate phase formation. These plates were observed in some Co free alloys after 24 hours of aging and in all Co free alloys after 100 hours of aging.

3. Removal of cobalt destabilized the MC type carbides resulting in massive breakdown of MC into $M_{23}C_6$ type carbides. Massive breakdown was observed in Co free samples as early as after 100 hours of aging.

4. Removal of cobalt increased grain boundary pre-

cipitation of $M_{23}C_6$ type carbides resulting in continuous films. Continuous films were observed in one Co free alloy after 24 hours of aging and in all Co free alloys after 100 hours of aging.

5. Cobalt containing alloys displayed more discrete and limited $M_{23}C_6$ formation in grain boundaries and in MC carbide breakdown. This observation was noted in all Co containing alloys at all stages of aging.

In the as cast Co free alloys, massive precipitation of discrete interdendritic $M_{23}C_6$ carbides was found, indicating more segregation within the grains. This segregation was not observed after the solutioning heat treatment. Figure 9 displays characteristic morphologies of plate formation, grain boundary $M_{23}C_6$, MC breakdown, and interdendritic $M_{23}C_6$ formation.

4.2 Mechanical Testing

Room temperature tensile and stress rupture tests were carried out on all twelve alloys having the standard commercial heat treatment. A summary of the test results as a function of each elemental variation is given in Table III.

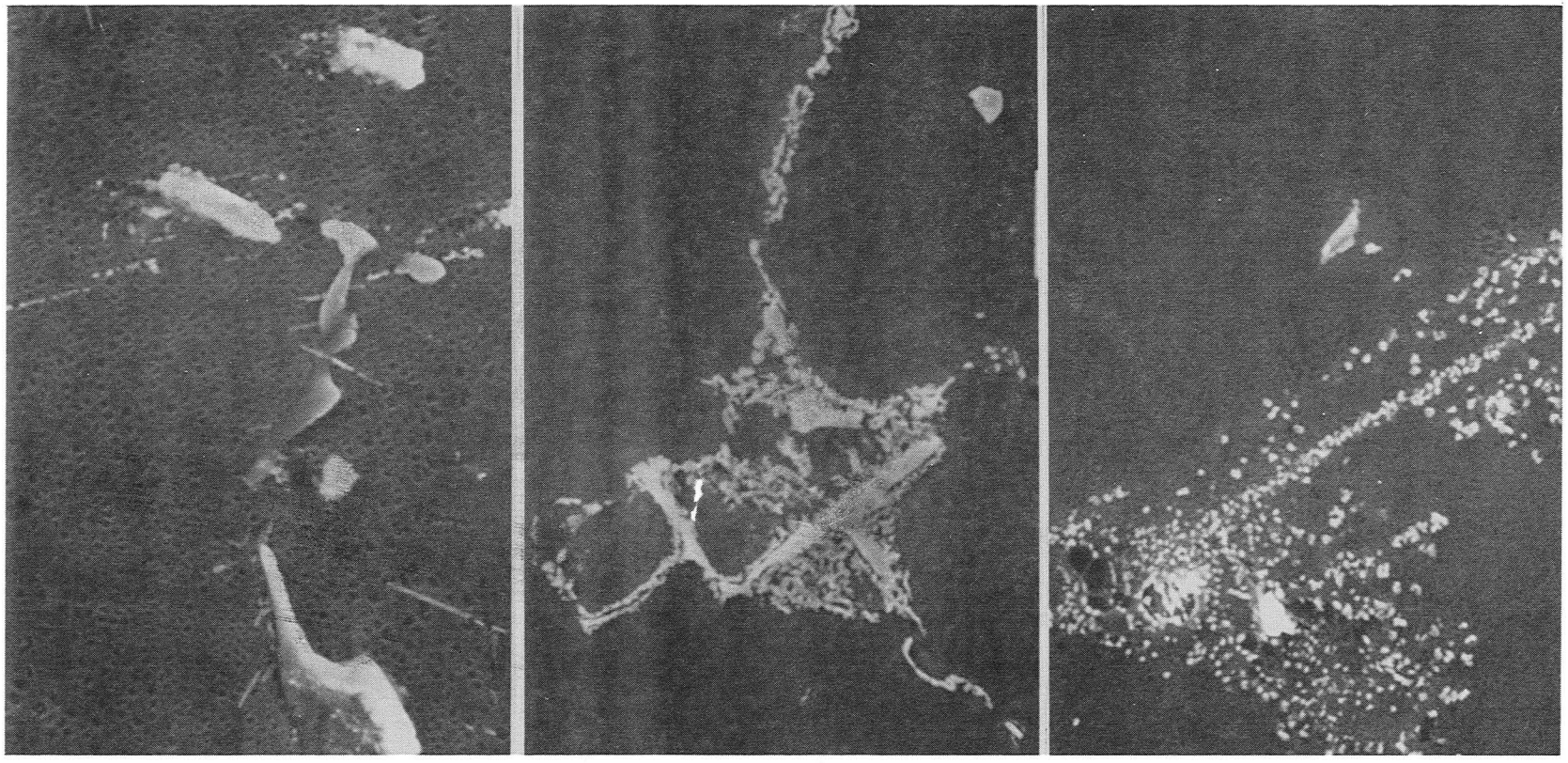

Figure 9. SEM Micrographs of LTA Samples. (a) Alloy 1B sltn. treated + aged 500Hrs. 1500X (b) Alloy 4A A.C. + aged 300Hrs. 1500X (c) Alloy 4A A.C. + aged 500Hrs. 2000X

TABLE III. Mechanical Property Test Results

Ambient Tensile					Stress Rupture	
Alloy	S_u(MPa)	S_y(MPa)	%Elong.	%R. of A.	Life	%Elong.
1A	1065	800	8.4	10.2	59	13.1
1B	1067	744	5.7	10.2	63	14.3
2A	1084	773	9.1	10.1	60	20.0
2B	1008	771	6.1	9.3	50	21.7
3A	996	761	6.1	10.2	59	16.7
3B	1005	770	6.0	8.7	43	17.0
4A	927	765	2.1	2.5	57	19.1
4B	1025	752	6.1	7.9	42	8.5
5A	990	765	5.9	9.3	39	8.0
5B	974	756	5.6	4.8	49	10.0
6A	1005	756	5.0	7.9	40	16.0
6B	965	762	5.0	7.2	31	11.0

Figure 10 shows the uniaxial tensile properties with respect to cobalt. Generally, alloys with cobalt had a +5.3% average improvement in ultimate strength over alloys without cobalt.

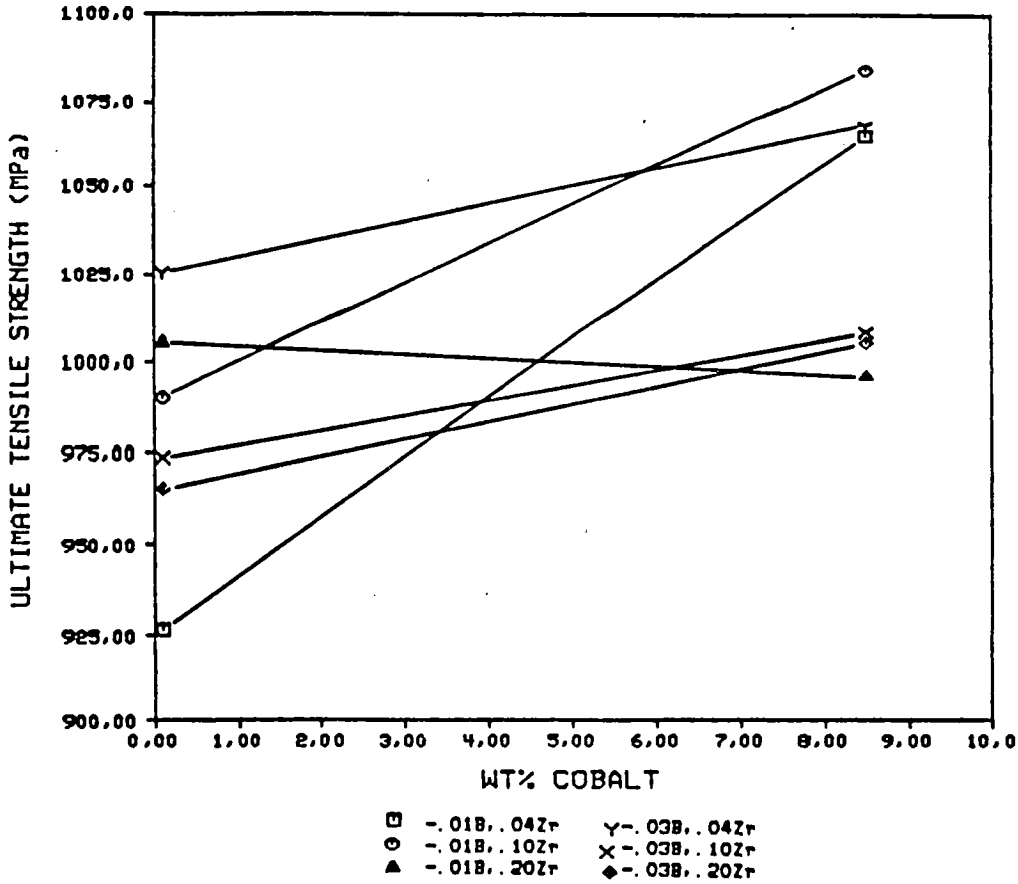

Figure 10. Ultimate Tensile Strength vs. Wt% Cobalt

Figure 11 shows the effect of boron on uniaxial tensile properties. Four of the six alloys in which boron was varied showed less than 5% change in ultimate strength from alloys with the standard level of boron. The other two exhibited opposite behaviors with larger changes in strength. Therefore it is difficult to correlate additions of boron to any trend in uniaxial tensile strength.

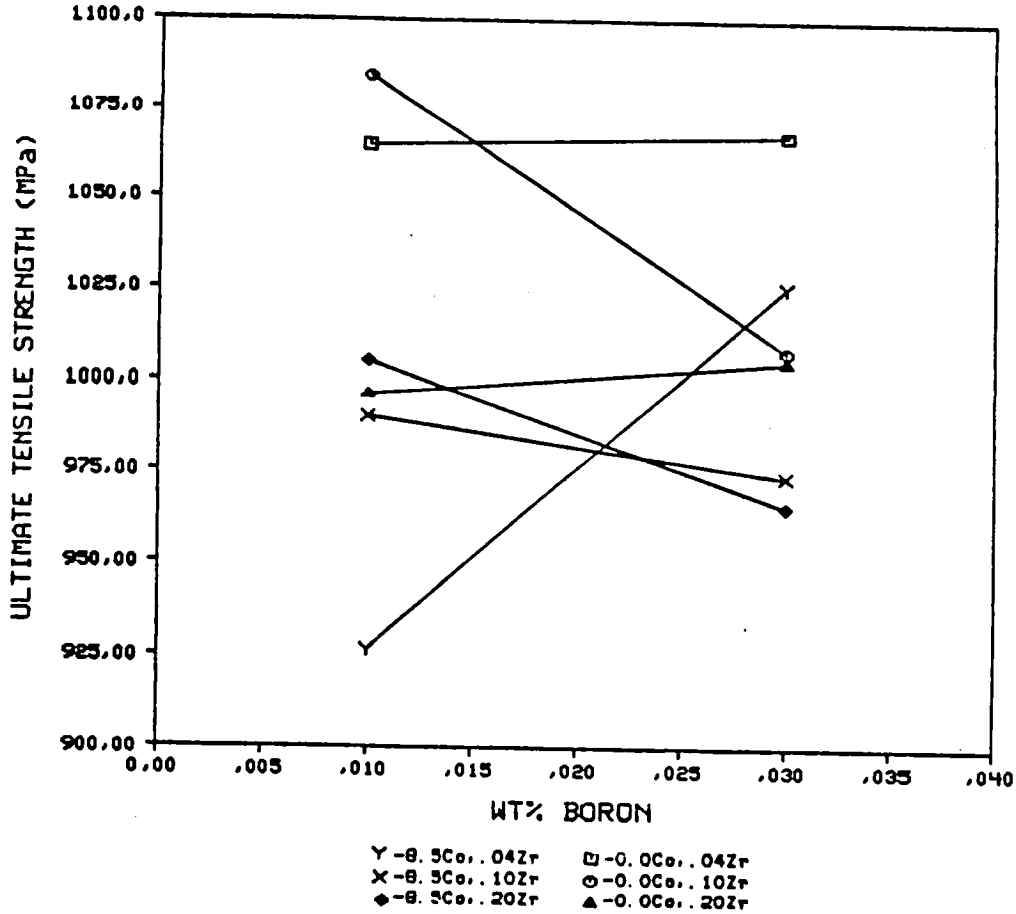

Figure 11. Ultimate Tensile Strength vs. Wt% Boron

Zirconium additions and their impact on ultimate strength are depicted in Figure 12. Overall there appeared to be a decrease in strength with increasing zirconium content. However, as with boron, it difficult to define a trend.

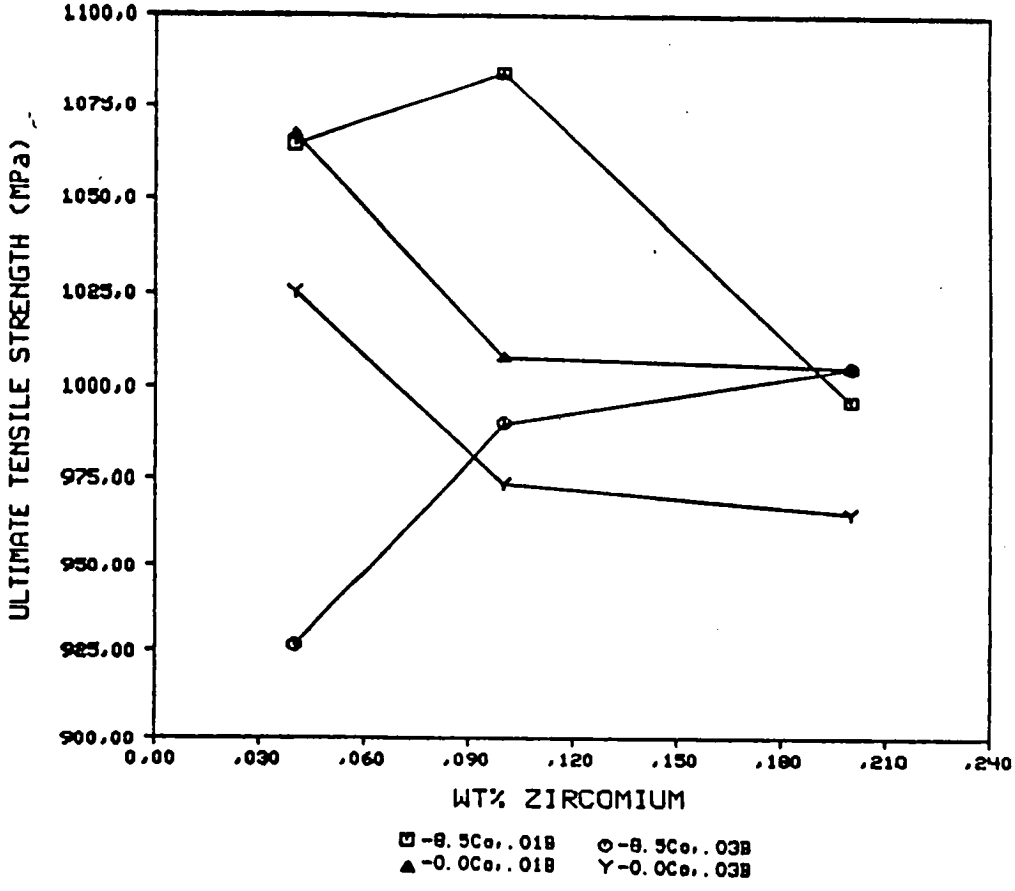

Figure 12. Ultimate Tensile Strength vs. Wt% Zirconium

Stress rupture lives were also plotted with respect to compositional variation, and again, cobalt alloys displayed an overall improvement in rupture life by +22% (see Figure 13).

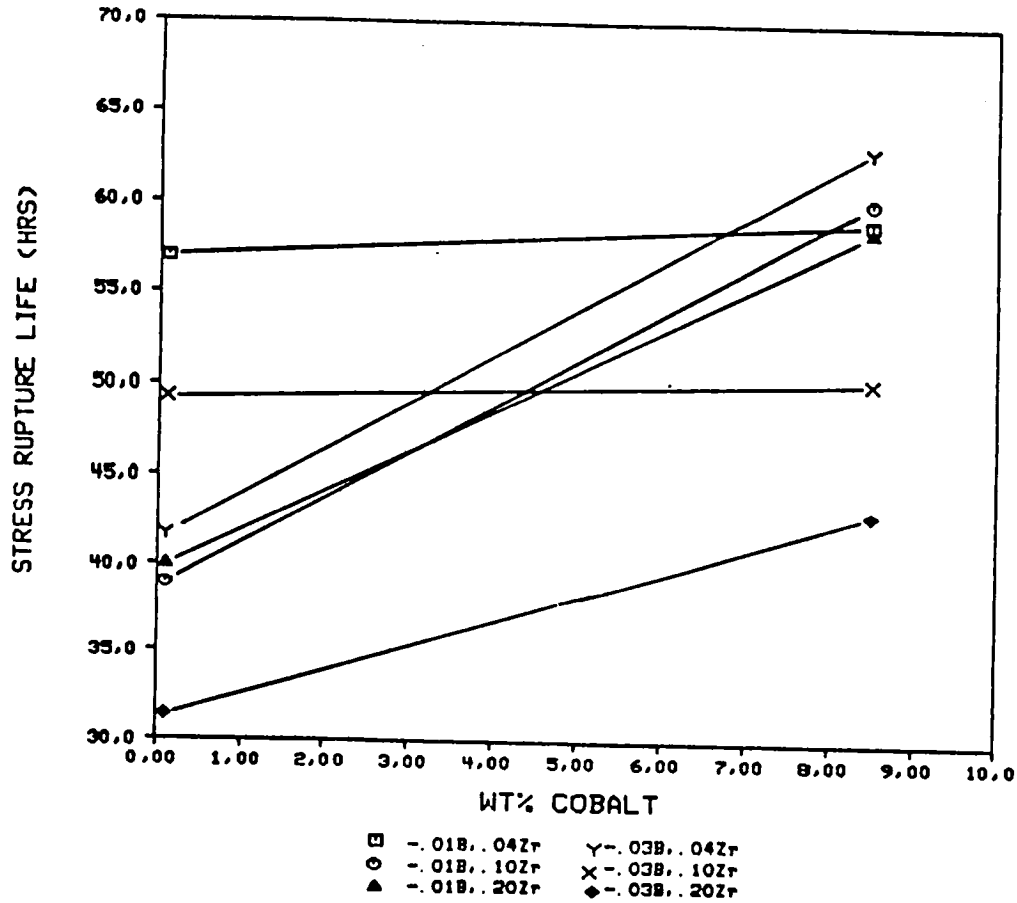

Figure 13. Stress Rupture Life vs. Wt% Cobalt

Boron additions seemed to decrease rupture life; however, two of the six alloys had significantly improved lives (see Figure 14).

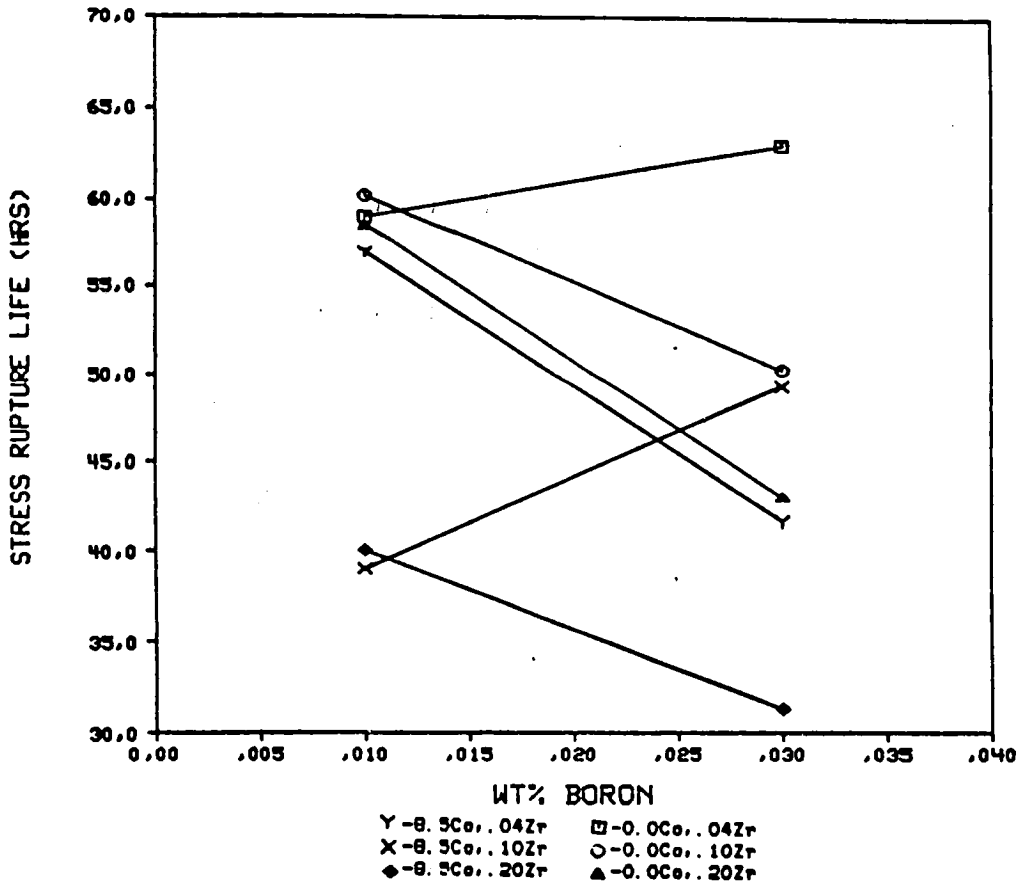

Figure 14. Stress Rupture Life vs. Wt% Boron

Zirconium additions also displayed an overall decrease in rupture life (Figure 15). Alloys with the .20 wt% level of zirconium consistently showed shorter rupture life as compared to the alloys with the .04 wt% level of zirconium.

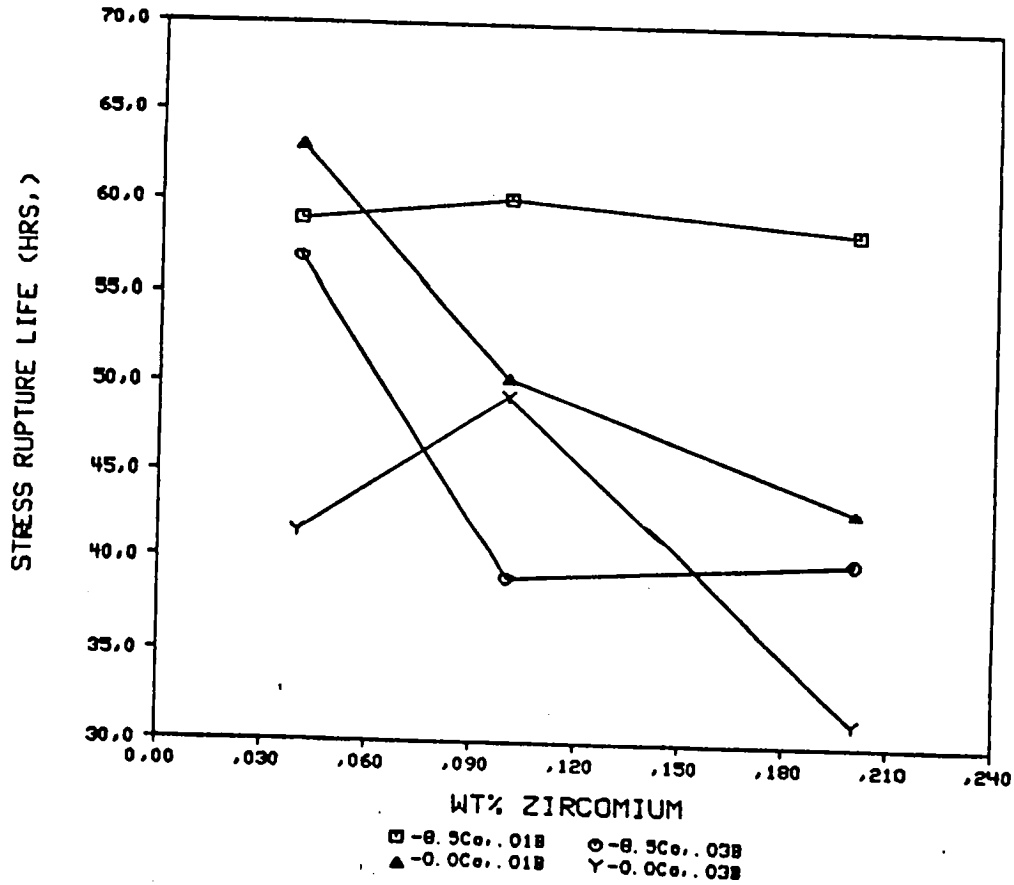

Figure 15. Stress Rupture Life vs Wt% Zirconium

The percent of elongation was used to compare ductility. Both tensile ductility and stress rupture ductility were plotted together relative to compositional variation.

Figure 16 depicts the effect of cobalt on ductility. Tensile ductility improved with cobalt additions at low boron levels and was constant at high boron levels. Rupture ductility showed mixed results, but there was a trend of improved ductility with the addition of cobalt, especially at high boron levels.

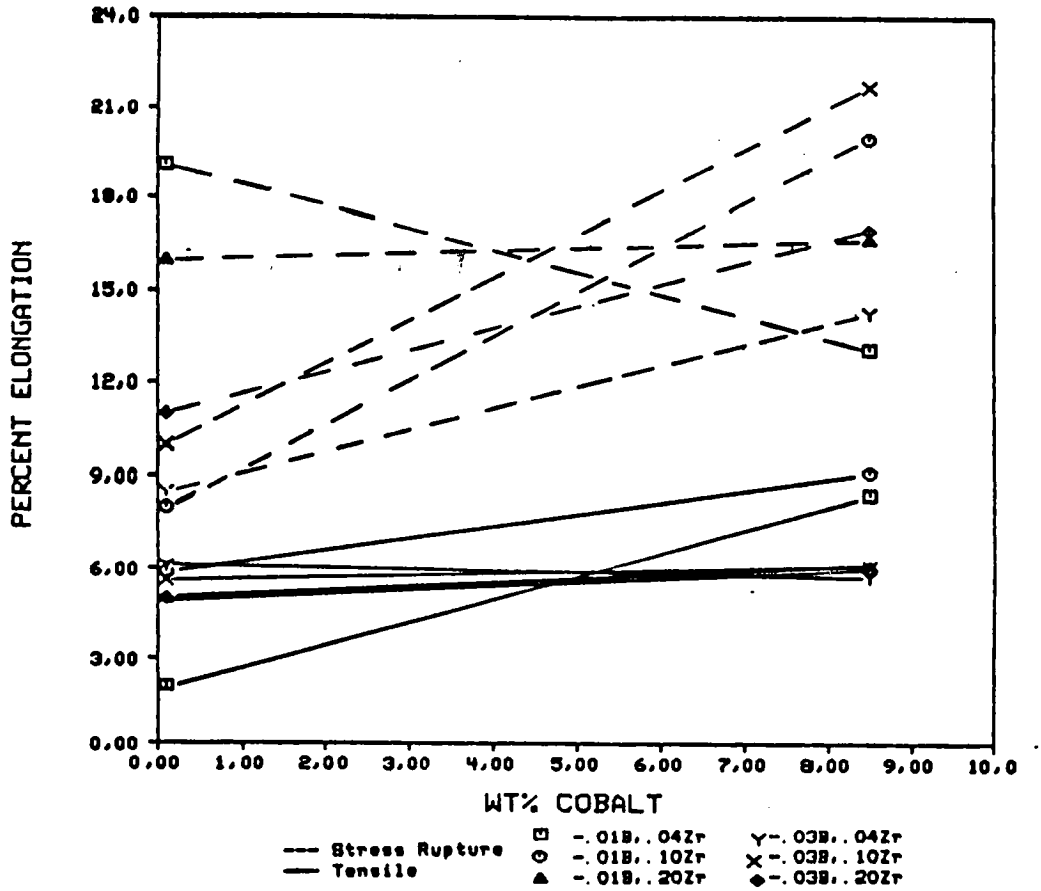

Figure 16. Percent Elongation vs. Wt% Cobalt

The effect of boron on ductility is shown in Figure 17. At room temperature the results again were mixed. Generally reduction in ductility occured with increased boron and Zr levels. At elevated temperatures, ductility was virtually constant when boron was increased and cobalt was present. Removal of cobalt and increased amounts of boron showed a general reduction in ductility.

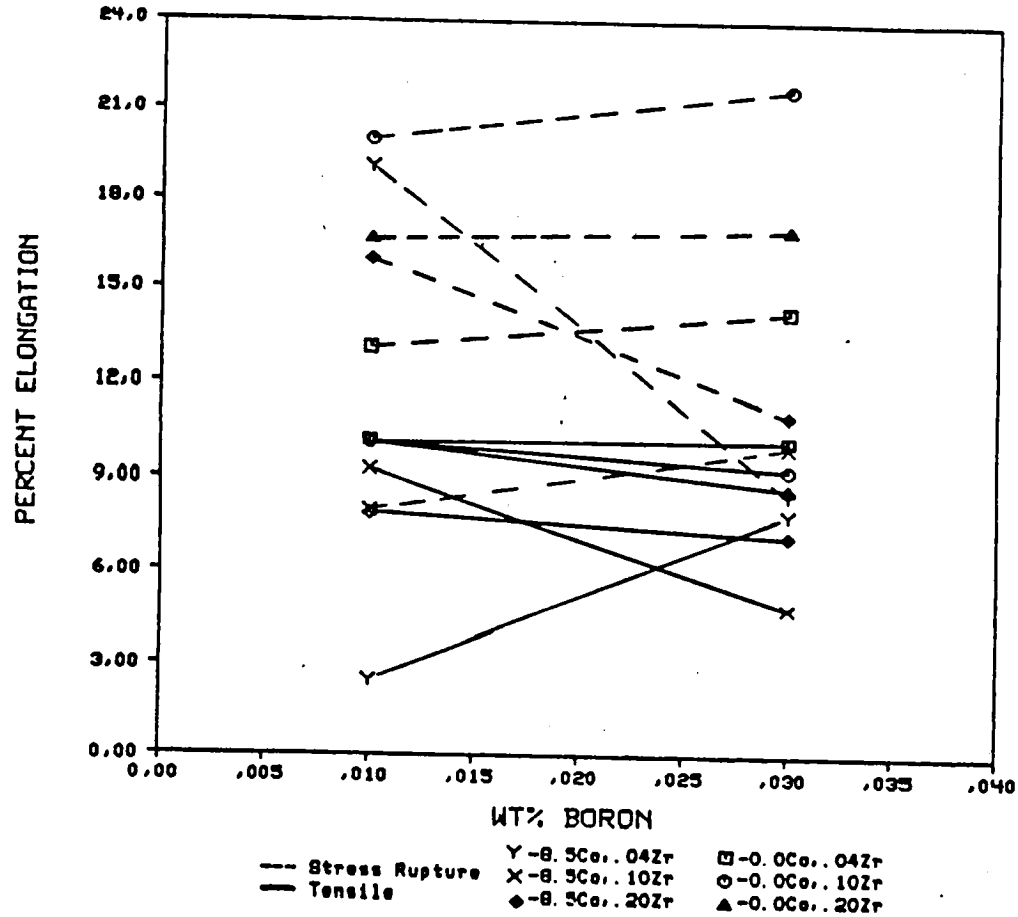

Figure 17. Percent Elongation vs. Wt% Boron

When zirconium was the variable, tensile ductility showed no trend. Rupture ductility showed general improvement although again the results were not consistent (Figure 18).

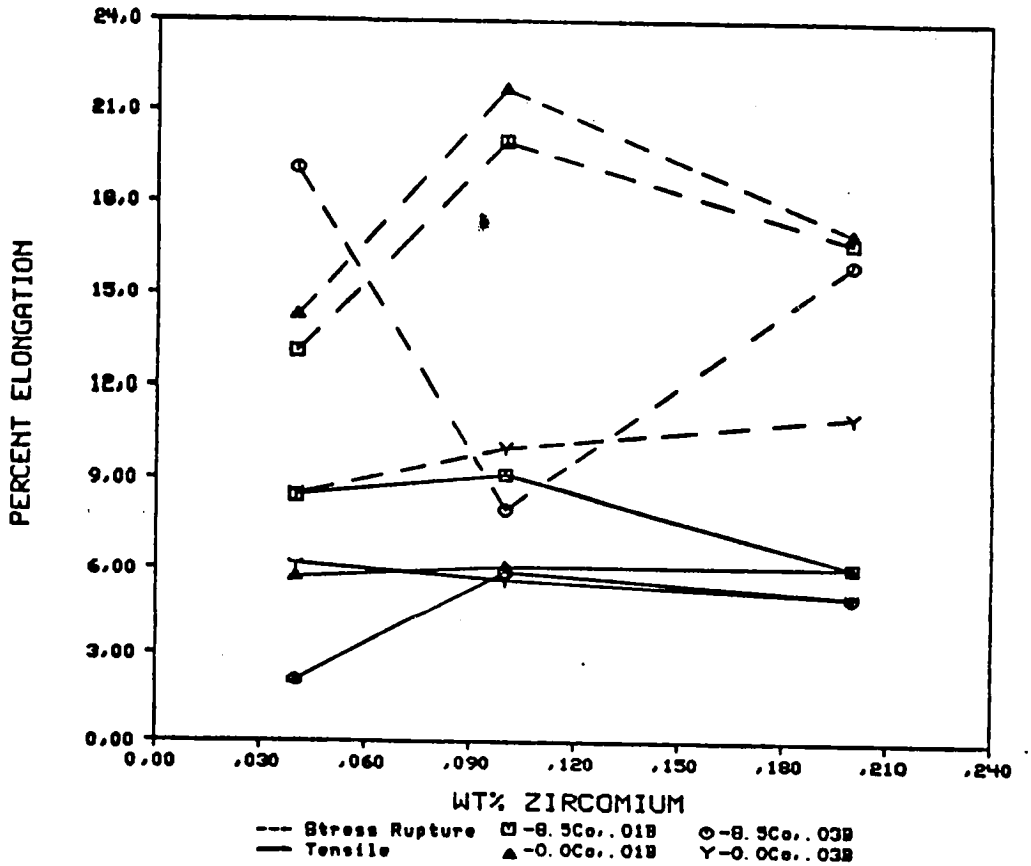

Figure 18 Percent Elongation vs. Wt% Zirconium

4.3 Fractography

Fractographic analysis failed to reveal any causes of failure that could explain the inconsistencies in mechanical properties. Although all samples showed varying degrees of porosity, it was concluded that porosity was not a major factor in failure. Large quantities of brittle MC carbide fracture were observed in many samples. All fractures were transgranular.

4.4 Phase Extraction Identification

The structures present in Udimet 738 were identified by X-ray powder diffraction analysis of extracted phases. Table IV shows the phases present in the coarse and fine residues extracted from the standard heat treated alloys.

The boride phase appeared only in the coarse residue of those alloys alloys with a high level of boron. The boride phase was found in the fine residues of all high level boron alloys as well as in the residues of low boron level alloys that did not contain cobalt. The $M_{23}C_6$ phase appeared to be greater in amount in Co free alloys. The amount of MC phase appeared fairly consistent and no shifts in lattice parameter were noted regardless of alloy composition.

TABLE IV. X-ray Peak Identification

Coarse Residue	Fine Residue
MC 4.36 Å	MC 4.36 Å
CrB_x (M_5B_3)	$M_{23}C_6$ 10.70 Å
	CrB_x (M_5B_3)

V. DISCUSSION OF RESULTS

5.1 Role Of Cobalt In U-738

Cobalt at levels of 8.5 wt% and 0 wt% displayed little direct interaction with boron and zirconium. For the most part, borides were script like in appearance in alloys containing cobalt and more massive when cobalt was removed. No cobalt borides were found.

Cobalt had a more profound effect on γ'. Alloys containing cobalt showed a duplex γ' structure after solutioning whereas alloys without Co did not. This indicated that the γ' solvus temperature has been raised by the removal of cobalt. This observation agrees with the results of studies by Engel[3], Nathal *et al*.[4], and Jarret and Tien.[6] It was difficult to determine optically if the volume fraction of γ' was altered by cobalt removal. The as cast γ' morphology in all alloys appeared similar in size and shape. Eutectic γ' islands in Co free alloys displayed less homogenization possibly indicating an increased solvus temperature.

Samples which had a duplex γ' structure showed an improvement in stress rupture properties. The increase in stress rupture results agrees with results reported previously.[5,6,9] Stress rupture improvement generally has been attributed to discrete grain boundary precipitation and γ'

volume fraction.[5] While cobalt prevented continuous films in the grain boundaries, it is not certain as to whether an increase in γ' volume fraction occurred.

Tensile properties have also been related to γ' morphology and discrete grain boundary carbides. Because the γ' particle size distribution and volume fraction were not measured, it is difficult to say which factor had the most significant influence on tensile properties, γ' or discrete carbides. In this study, alloys containing Co showed an improvement in tensile properties, whereas published literature has reported little or no tensile property improvement.

Cobalt stabilized the MC carbides by preventing MC breakdown thereby inhibiting massive $M_{23}C_6$ formation in the grain boundaries. Many studies agree with this result.[3,6,7,9] In long time aged samples of 500 hours, cobalt apparently retarded σ formation. This does not agree with earlier reports by Engel[3] and Lund et al;[8] however, their studies were on alloys of different composition than U-738.

5.2 Effect Of Boron

Many claims have been made as to the beneficial effects of boron. Most studies report grain boundary effects including carbon shunting and complex oxide retardation. In this study of U-738, B additions did not alter the grain

boundary morphology. In comparison of low B alloys to high B alloys, the $M_{23}C_6$ carbide precipitation and as cast γ' showed no change in quantity or shape. to high B alloys. The most notable effects of higher boron additions appeared as the formation of a large boride phase and increased size and amount of eutectic γ' islands. The boride phase was most often found near these eutectic islands and rarely appeared in the grain boundaries. Most significantly, B additions did not result in an improvement in mechanical properties, but rather a decrease in stress rupture life was found. This does not coincide with findings by Holt and Wallace[12], Decker and Freeman[13], and Antony and Radavich;[11] however, their studies considered levels of boron primarily in the range of 0.0 wt% to .01 wt%, whereas this study compared B levels of .01 to .03 wt%. This suggests that addition of B beyond the .01 wt% level may be ineffective in increasing mechanical properties of Udimet 738. Since the solid solubility limit of B in pure Ni is approximately .015 wt%, higher levels of B may only result in the formation of larger borides which do not contribute to mechanical properties.

5.3 Effects Of Zirconium

Zirconium is a trace element which may control grain boundary precipitation and act as a getter of sulphur, thereby improving high temperature strength and ductility.

Zr has been reported to have a homogenizing effect on γ' and to promote discrete and less numerous MC carbides.[19] Results of this study showed that samples of high Zr level had as cast γ' which appeared more uniform in size and shape. Solution treated alloys with high Zr levels also showed a duplex γ' structure that was not as distinct as that seen in alloys with low Zr levels. The ultrafine secondary γ' appeared more dispersed in the matrix of high Zr level alloys. Zr additions showed no effect on MC morphology.

Zr additions also increased the size and quantity of eutectic γ' islands which agrees with previous studies.[11,19] Zr appeared to be heavily segregated at eutectic γ' islands as the majority of Zr rich stick phases were found in these areas. Grain boundary morphology appeared unaffected by Zr additions.

In this study, the effects of Zr on mechanical properties showed mixed results and it was difficult to observe any trends. Holt and Wallace reported that rupture life and ductility were independent of Zr content in alloy 738 and thus the beneficial effects of Zr may be alloy dependent.[12] In the study of Antony and Radavich, Zr had an adverse effect on mechanical properties which was attributed to microporosity. Their samples were taken from integrally cast wheels in which the microporosity was more dependent on changes in the solidification range. Samples in this study

were cast to size test bars in which solidification was very rapid, thereby decreasing the effects of a large solidification range. Yet microporosity was observed in the tested bars. However, no correlation of porosity to mechanical properties or Zr level could be made.

VI. CONCLUSIONS AND RECOMENDATIONS

6.1 Conclusions

Variations of the minor elements B and Zr with the major alloying element cobalt resulted in changes in microstructure and although the complete role of cobalt is not fully understood in U-738, some of the effects of cobalt are as follows:

1. The presence of cobalt did not affect the as cast γ' morphology.
2. Removal of cobalt increased the γ' solvus temperature.
3. The amount of secondary γ' was decreased after solution treatment in Co free alloys.
4. A decrease in stress rupture properties was associated with the loss of secondary γ'.
5. Removal of cobalt promoted $M_{23}C_6$ precipitation.
6. Cobalt stabilized primary MC carbides.
7. Cobalt inhibited formation of continuous grain boundary films.
8. Cobalt helped to prevent σ formation.

Boron and zirconium had the following effects:

1. Boron additions beyond .01 wt% precipitated large borides without a substantial change in mechanical properties.
2. Zirconium additions created subtle changes in γ'

but did not effect mechanical properties.

3. High Zr levels promoted Zr rich stick phase precipitation near eutectic γ′ islands.
4. Boron and zirconium had little effect on matrix carbides or the morphology of grain boundary carbides.
5. Boron and zirconium increased the solidification range of the alloy which resulted in larger and more numerous eutectic γ′ islands.
6. Within the scope of this study of cast to size bars, there was no correlation between porosity and B plus Zr content, although porosity was observed in some fracture surfaces.

6.2 Recommendations

The results of this study showed that additional research needs to be done to answer the difference in results found in this study compared to results reported in the referenced literature. The following areas for future research are recommended:

1. Because of the great degree of difference in castability of cast to size test bars and large cast components, it is recommended that actual components be cast with the compositional variations used in this study and evaluate the effects of B and Zr on porosity formed during solidification.

2. More mechanical property tests should be performed to insure statistical reliability.
3. Larger variations in composition, notably B and Zr in U-738, should be investigated to determine the extreme amounts of B and Zr which would be acceptable in this alloy.

LIST OF REFERENCES

1. C.T. Sims, W.C. Hagel, The Superalloys, John Wiley and Sons Inc., New York, 1972.

2. D.R. Betner, K.E. Muszar, E.S. Nichols, "Phase Stability of Two Investment Cast High Cr Ni-Base Alloys", Procedings of the First International Symposium on Structural Stability in Superalloys Seven Springs, Penn., pp. 278-311, 1968.

3. M.A. Engel, "Effects Of Co On The Microstructure Of U-700", M.S. in Metallurgical Engr. Thesis, Purdue Univ., 1981.

4. M.V. Nathal, R.D. Maier, L.J. Ebert, "The Influence Of Co On The Microstructure Of The Ni-Base Superalloy MAR-M247", Metallurgical Transactions, pp. 1775-1783, Oct. 1982.

5. M.V. Nathal, R.D. Maier, L.J. Ebert, "The Influence Of Co On The Tensile And Stress Rupture Properties Of The Ni-Base Superalloy MAR M247", Metallurgical Transactions, pp. 1767-1774, Oct. 1982.

6. R.N. Jarret, J.K. Tien, "Effects Of Co On Structure, Microchemistry, And Properties Of A Wrought Ni-Base Superalloy", Metallurgical Transactions, pp. 1021-1032, June 1982.

7. J. Heslop, "Wrought Ni-Cr Heat Resisting Alloys Containing Cobalt", Cobalt, Vol. 24, pp. 128, Sept. 1964.

8. C.H. Lund, M.J. Woulds, J. Hockin, "Cobalt And Sigma: Participant, Spectator, or Referee?", Procedings of the First International Symposium on the Structural Stability in Superalloys, Seven Springs, Penn., pp. 25-46, 1968.

9. G.E. Mauer, L.A. Jackman, J.A. Domingue, "Role Of Cobalt In Waspaloy", Superalloys 1980, Procedings of the Forth International Symposium on Superalloys, Champion, Penn., pp. 43-52, 1980.

10. E.P. Whelan, "Co-Free Ni-Base Wrought Superalloys", Superalloys 1980, pp. 53-62, 1980.

11. K.C. Antony, J.F. Radavich, "Solute Effects of B and Zr on Microporosity", Technical paper, Cabot Corp., Kokomo, Ind.

12. R.T. Holt, W. Wallace, "Impurties And Trace Elements In Ni-Base Superalloys", International Metals Review, pp. 1-23, March 1976.

13. R.F. Decker, J.W. Freeman, "The Mechanism Of Beneficial Effects Of B And Zr On Creep Properties Of A Complex Heat Resistant Alloy", Transactions of the Metallurgical Society of AIME, vol. 218, pp 277-285, April 1960.

14. B. Hu, H. Li, "Neutron Activated Microradiography Determination Of Boron Distribution Of A Cast Ni-Base Superalloy", Superalloys 1980, pp. 423-429, 1980.

15. D.A. Woodford, "Environmental Damage Of A Cast Ni-Base Superalloy", Metallurgical Transactions, pp. 299-308, Feb. 1981.

16. D.A. Woodford, R.H. Bricknell, "Grain Boundary Penetration Of Oxygen In Nickel And The Effect Of B Additions", Metallurgical Transactions, pp. 1467-1475, August 1981.

17. S. Floreen, J.M. Davidson, "The Effects Of B and Zr On The Creep And Fatigue Crack Growth Behavior Of A Ni-Base Superalloy", Metallurgical Transactions, pp. 895-901, May 1983.

18. K.N. Strafford, B.A. Nagaraj, "Degredation Of Zr Containing Ni-Base Alloys In A Hydrogen/Hydrogen-Sulfide Environment", Oxidation of Metals, vol. 14, no. 2, pp. 109-117, 1980.

19. J.F. Radavich, "Effects Of Zr Variations On The Microstructural Stability Of Alloy 713C", Procedings of the First International Symposium on the Structural Stability of Superalloys, Seven Springs, Penn., pp. 199-226, 1968.

20. Y. Koizumi, M. Yamazaki, H. Harada, "M_5B_3 Type Boride In Nickel-Base Superalloys", Transactions of National Research Institute For Metals, vol. 19, no. 6, pp. 60-61, 1977.

APPENDIX A

Sample Preparation And Examination

Sample Preparation

Samples used in this study were taken from cast to size test bars that had experienced all levels of heat treatment and long time aging (LTA). Aging periods were 100, 300, and 500 hours at 843°C. Both the solution treated and as cast samples were exposed to LTA. The cast to size bars were severed in the test region, then ground flat longitudinally. Each sample was then wet ground through 600 grit silicon carbide followed by an electropolish in 20% sulfuric acid in methanol electrolyte solution. A stainless steel beaker served as the cathode and the sample itself as the anode. The polishing parameters were 20 volts, 3 to 5 amps for approximately 8 seconds. This was followed immediately by an immersion etch in a 15% hydrochloric acid in methanol plus a few drops of 30% hydrogen peroxide solution for 5 to 10 seconds.

The electropolish served to put the carbides, borides, TCP, and other inert phases in relief. MC carbides that are rich in titanium should appear black in the scanning electron microscope due to the relatively low atomic weight of titanium. Other inert phases should appear either gray or bright. The immersion etch removes the γ' phase, resulting

in three different levels of microstructure. The etched γ' should appear dark, since it is at the lowest level, the γ matrix should appear gray (intermediate level), and the carbides and inert phases at the top level are as previously described. The etching of the γ' and grain boundaries acts to enhance the contrast of each sample.

Microstructural and Chemical Analysis

Microstructures of each sample were characterized with a J. E. O. L. JSM 35CF scanning electron microscope (SEM). The various morphologies and locations of the phases present were recorded electon micrographically. An energy dispersive X-ray analyzer (EDAX), attached to the SEM was used to aid in phase composition analysis. Spot probing allowed for a general qualitative analysis of phases in situ..

Phase Extractions and Identification

Isolation of phases other than the matrix and γ' were required for positive identification. A standard electrolytic extraction technique was employed for the removal of the inert boride, carbide, and TCP phases. Extraction samples were supplied from the remaining half of the severed cast to size test bars used in the SEM study. A 10% hydrochloric acid in methanol electrolyte, tantalum cathode, and extraction sample as anode were operated on the basis of .07

amps per square centimeter of anode. Extraction time lasted approximately 1 hour. The residue was periodically washed from the extraction sample in clean methanol and was allowed to settle a minimum of 12 hours before separation and filtering. The extracted residues were agitated until fully suspended. Settling was permitted for three minutes at which time all the methanol was decanted off and placed in a separate container. Additional clean methanol was added to the remaining settled residue and the agitation-separation process repeated. The decanted methanol held a suspended fine residue while the remaining residue was defined as coarse. Each residue was then filtered from the methanol using Millipore .6 micron filter papers. The filter papers were then mounted on glass slides in preparation for X-ray identification.

The extracted and mounted residues were subjected to powder diffraction analysis to identify the fine and coarse residues in each alloy. A General Electric X-ray diffractometer was used to generate the diffraction patterns with nickel filtered copper K_{α} radation. The parameters used were 40 KV, 20 ma for primary X-ray excitation. Scanning range was from 25 to 61^{o} 2θ.

APPENDIX B

FORM 2242-T (REV.6-74)

MATERIALS RESEARCH LABORATORY

DETROIT DIESEL ALLISON DIVISION OF GENERAL MOTORS

SHORT-TIME ELEVATED TEMPERATURE TENSION TEST REPORT

PROJECT NO. PURDUE ST. CHARGE NO. P6E-100 EDO NO. P.6E.H.
MATERIAL / SPECIFICATION IN 738 SOURCE J. HECKLER
TESTING MACHINE EXTENSOMETER
DATE 12/20/83 OPERATOR

1. RECORD OF TEMPERATURE CONTROL

SPECIMEN NO.	1A	1B	2A	2B	3A	3B	4A	4B
CONTROL TEMP., CENTER OF SPECIMEM, °F	RT							→
Instron	1505	1506	1507	1508	1509	1510	1511	1512

2. OBSERVED DATA OF SHORT-TIME ELEVATED TEMPERATURE TENSION TESTS

SPEED OF HEAD OF TESTING MACHINE UP TO REMOVAL OF EXTENSOMETER, IN. PER MIN.								
SPEED OF HEAD OF TESTING MACHINE AFTER REMOVAL OF EXTENSOMETER, IN. PER MIN.								
ORIGINAL DIAMETER OF SPECIMEN, IN.	.250	.250	.251	.250	.249	.250	.247	.251
FINAL DIAMETER OF SPECIMEN, IN.	.237	.237	.238	.238	.236	.239	.244	.241
ORIGINAL C/S AREA, IN.^{2}	.0491	.0491	.0495	.0491	.0487	.0491	.0479	.0495
FINAL C/S AREA, IN.^{2}	.0441	.0441	.0445	.0445	.0437	.0448	.0467	.0453
DIFF. C/S. AREA, IN.^{2}	.0050	.0050	.0050	.0046	.0050	.0043	.0012	.0042
ORIGINAL WIDTH, IN.								
ORIGINAL THICKNESS, IN.								
ORIGINAL C/S AREA, IN.^{2} Y.L.	5696	5512	5548	5488	5372	5480	5312	5400
MAXIMUM LOAD, LB.	7580	7600	7780	7180	7040	7160	6440	7360
ELONGATION, FINAL LENGTH, IN.	1.084	1.057	1.091	1.061	1.061	1.060	1.021	1.061
ORIGINAL LENGTH, IN.	1.000	1.000	1.000	1.000	1.000	1.000	1.000	1.000
ELONGATION LENGTH, IN.	.084	.057	.091	.061	.061	.060	.021	.061
LOCATION OF FRACTURE		B.O.G.					B.O.G.	

	1A	1B	2A	2B	3A	3B	4A	4B
3. CALCULATED RESULTS OF SHORT-TIME ELEVATED-TEMPERATURE TENSION TESTS								
TENSILE STRENGTH, psi	154.4	154.8	157.2	146.2	144.5	145.8	134.4	148.7
YIELD STRENGTH, (0.2% OFFSET) psi	116.0	112.2	112.1	111.8	110.3	111.6	110.9	109.1
(0.02% OFFSET) psi								
ELONGATION PERCENT	8.4	5.7	9.1	6.1	6.1	6.0	2.1	6.1
REDUCTION OF AREA, PERCENT	10.2	10.2	10.1	9.3	10.2	8.7	2.5	7.9
ODULUS OF ELASTICITY, 10^6 psi								

FORM 2242-T (REV.6-74)

MATERIALS RESEARCH LABORATORY

DETROIT DIESEL ALLISON DIVISION OF GENERAL MOTORS

SHORT-TIME ELEVATED TEMPERATURE TENSION TEST REPORT

PROJECT NO. Purdue Student CHARGE NO. P.6610 EDO NO.
MATERIAL / SPECIFICATION IN 738 SOURCE J. Hecklerc
TESTING MACHINE EXTENSOMETER
DATE 12/20/83 OPERATOR

1. RECORD OF TEMPERATURE CONTROL

SPECIMEN NO.	5A	5B	6A	6B				
CONTROL TEMP, CENTER OF SPECIMEM, °F	→	→	→	→				
Setpoint	1513	1514	1515	1516				

2. OBSERVED DATA OF SHORT-TIME ELEVATED TEMPERATURE TENSION TESTS

SPEED OF HEAD OF TESTING MACHINE UP TO REMOVAL OF EXTENSOMETER, IN. PER MIN.								
SPEED OF HEAD OF TESTING MACHINE AFTER REMOVAL OF EXTENSOMETER, IN. PER MIN.								
ORIGINAL DIAMETER OF SPECIMEN, IN.	.254	.248	.250	.249				
FINAL DIAMETER OF SPECIMEN, IN.	.242	.239	.240	.240				
ORIGINAL C/S AREA, IN.^{2}	.0507	.0483	.0491	.0487				
FINAL C/S AREA, IN.^{2}	.0460	.0448	.0452	.0452				
DIFF. C/S. AREA, IN^2	.0047	.0035	.0039	.0035				
ORIGINAL WIDTH, IN.								
ORIGINAL THICKNESS, IN.								
ORIGINAL C/S AREA, IN.^{2} Y.L	5624	5296	5384	5380				
MAXIMUM LOAD, LB.	7280	6820	7160	6820				
ELONGATION, FINAL LENGTH, IN.	1.059	1.056	1.050	1.050				
ORIGINAL LENGTH, IN.	1.000	1.000	1.000	1.000				
ELONGATION LENGTH, IN.	.059	.056	.050	.050				
LOCATION OF FRACTURE								

	5A	5B	6A	6B				
3. CALCULATED RESULTS OF SHORT-TIME ELEVATED-TEMPERATURE TENSION TESTS								
TENSILE STRENGTH, psi	143.6	141.2	145.8	140.0				
YIELD STRENGTH, (0.2% OFFSET) psi	110.9	109.6	109.6	110.5				
(0.02% OFFSET) psi								
ELONGATION PERCENT	5.9	5.6	5.0	5.0				
REDUCTION OF AREA, PERCENT	9.3	4.8	7.9	7.2				
MODULUS OF ELASTICITY, 10^6 psi								

FORM 2273

INDEX NO. 1608

CREEP – RUPTURE REPORT

PROJ. NO. PROTOTYPE SPECIMEN NO. 1A CHG. NO. P.661 DATE 12/20/83

REQUESTED BY J. HAROLD MACHINE NO. 1

MATERIAL SPECIFICATION OR ALLOY IN 738

CONDITION

STRESS RUPTURE ✓ CREEP TEST

TEST TEMPERATURE 1700 STRESS 22.0 KSI

OTHER INFORMATION OR REMARKS

DIAMETER .250 "

LOAD-PAN (20:1 BEAM 54.01 #

LOAD-SPECIMEN 1080.2 #

FINAL GAGE 1.131 "

ORIG. GAGE 1.000 "

DIFF. .131 "

ELONG. 13.1 %

DIAL GAGE-START

DIAL GAGE-STOP

DIFF.

ELONG. %

TIME OF DAY

INCREASE TO AT

INCREASE TO AT

INCREASE TO AT

INCREASE TO AT

TIMER READ.-FAIL OR STOP 4138.2

TIMER READING-START 4078.9

TEST TIME-HOURS 59.3

1/31:54

CREEP DATA:

FAILURE TYPE

NORMAL	✓
FAILED IN RADIUS	
FAILED OUTSIDE GAGE	
FAILED IN NOTCH	
FAILED IN THREADS	

FORM 2273

INDEX NO. 1609

CREEP – RUPTURE REPORT

PROJ. NO. RUNOUT STUDY SPECIMEN NO. 1B CHG. NO. P.GEN DATE 12/20/83

REQUESTED BY J. HECKLER MACHINE NO. 4

MATERIAL SPECIFICATION OR ALLOY IN738

CONDITION

STRESS RUPTURE ✓ CREEP TEST

TEST TEMPERATURE 1800 STRESS 22.0KSI

OTHER INFORMATION OR REMARKS

DIAMETER .249 "

LOAD-PAN (20:1 BEAM 53.57 #

LOAD-SPECIMEN 1071.4 #

FINAL GAGE 1.143 "

ORIG. GAGE 1.000 "

DIFF. .143 "

ELONG. 14.3 %

DIAL GAGE-START

DIAL GAGE-STOP

DIFF.

ELONG. %

TIME OF DAY

INCREASE TO AT

INCREASE TO AT

INCREASE TO AT

INCREASE TO AT

TIMER READ.-FAIL OR STOP 9592.8

TIMER READING-START 9529.8

TEST TIME-HOURS 63.0

11/31/84

CREEP DATA:

FAILURE TYPE

NORMAL	✓
FAILED IN RADIUS	
FAILED OUTSIDE GAGE	
FAILED IN NOTCH	
FAILED IN THREADS	

FORM 2273

INDEX NO. 1612

CREEP – RUPTURE REPORT

PROJ. NO. Ludlum St. SPECIMEN NO. 2X CHG. NO. P.6241 DATE 12/23/03

REQUESTED BY J. HOKLER MACHINE NO. 7

MATERIAL SPECIFICATION OR ALLOY INCO 7

CONDITION

STRESS RUPTURE ✓ CREEP TEST

TEST TEMPERATURE 1800 STRESS 22.0 KSI

OTHER INFORMATION OR REMARKS

DIAMETER .247 "

LOAD-PAN (20:1 BEAM 52.69 #

LOAD-SPECIMEN 1052.8 #

FINAL GAGE 1.206 "

ORIG. GAGE 1.000 "

DIFF. .206 "

ELONG. 20.0 %

DIAL GAGE-START

DIAL GAGE-STOP

DIFF.

ELONG. %

TIME OF DAY

INCREASE TO AT

INCREASE TO AT

INCREASE TO AT

INCREASE TO AT

TIMER READ-FAIL OR STOP 0376.2

TIMER READING-START 0316.0

TEST TIME-HOURS 60.2

1/3/04

CREEP DATA:

FAILURE TYPE

NORMAL	✓
FAILED IN RADIUS	
FAILED OUTSIDE GAGE	
FAILED IN NOTCH	
FAILED IN THREADS	

FORM 2273

INDEX NO. 1613

CREEP – RUPTURE REPORT

PROJ. NO. [illegible] SPECIMEN NO. 2B CHG. NO. [illegible] DATE 1/4/84

REQUESTED BY J. HICKLIN MACHINE NO. 1

MATERIAL SPECIFICATION OR ALLOY IN738

CONDITION

STRESS RUPTURE ✓ CREEP TEST

TEST TEMPERATURE 1800 STRESS 22.0 KSI

OTHER INFORMATION OR REMARKS

DIAMETER .250 "

LOAD-PAN (20:1 BEAM 54.01 #

LOAD-SPECIMEN 1080.2 #

FINAL GAGE 1.217 "

ORIG. GAGE 1.000 "

DIFF. .217 "

ELONG. 21.7 %

DIAL GAGE-START

DIAL GAGE-STOP

DIFF.

ELONG. %

TIME OF DAY

INCREASE TO AT

INCREASE TO AT

INCREASE TO AT

INCREASE TO AT

TIMER READ-FAIL OR STOP 4193.5

TIMER READING-START 4143.7

TEST TIME-HOURS 50.3

1/10/83

CREEP DATA:

FAILURE TYPE

NORMAL	✓
FAILED IN RADIUS	
FAILED OUTSIDE GAGE	
FAILED IN NOTCH	
FAILED IN THREADS	

FORM 2273

INDEX NO. 1614

CREEP – RUPTURE REPORT

PROJ. NO. [illegible] SPECIMEN NO. 3R CHG. NO. P.6[illegible] DATE 1/4/[illegible]

REQUESTED BY J. [illegible] MACHINE NO. 7

MATERIAL SPECIFICATION OR ALLOY IN 738

CONDITION

STRESS RUPTURE ✓ CREEP TEST

TEST TEMPERATURE 1800 STRESS 22.0 KSI

OTHER INFORMATION OR REMARKS

DIAMETER .250 "

LOAD-PAN (20:1 BEAM 54.01 #

LOAD-SPECIMEN 1080.2 #

FINAL GAGE 1.167 "

ORIG. GAGE 1.000 "

DIFF. .167 "

ELONG. 16.7 %

DIAL GAGE-START

DIAL GAGE-STOP

DIFF.

ELONG. %

TIME OF DAY

INCREASE TO AT

INCREASE TO AT

INCREASE TO AT

INCREASE TO AT

TIMER READ-FAIL OR STOP 04397

TIMER READING-START 0381.-

TEST TIME-HOURS 58.5

11,[illegible]5

CREEP DATA:

FAILURE TYPE

NORMAL	✓
FAILED IN RADIUS	
FAILED OUTSIDE GAGE	
FAILED IN NOTCH	
FAILED IN THREADS	

FORM 2273

INDEX NO. 1615

CREEP – RUPTURE REPORT

PROJ. NO. [illegible] SPECIMEN NO. 3B CHG. NO. P.6E.1. DATE 1/4/74

REQUESTED BY J. HALL MACHINE NO. 4

MATERIAL SPECIFICATION OR ALLOY IN 738

CONDITION

STRESS RUPTURE ✓ CREEP TEST

TEST TEMPERATURE 1800 STRESS 22 KSI

OTHER INFORMATION OR REMARKS

DIAMETER .250 "

DAD-PAN (20:1 BEAM 54.01 #

LOAD-SPECIMEN 1070.2 #

FINAL GAGE 1.170 "

ORIG. GAGE 1.000 "

DIFF. .170 "

ELONG. 17.0 %

DIAL GAGE-START

DIAL GAGE-STOP

DIFF.

ELONG. %

TIME OF DAY

INCREASE TO AT

INCREASE TO AT

INCREASE TO AT

INCREASE TO AT

TIMER READ.-FAIL OR STOP 9640.6

TIMER READING-START 9597.6

TEST TIME-HOURS 43.0

1/1.915

CREEP DATA:

FAILURE TYPE

NORMAL	✓
FAILED IN RADIUS	
FAILED OUTSIDE GAGE	
FAILED IN NOTCH	
FAILED IN THREADS	

FORM 2273

INDEX NO. 1610

CREEP – RUPTURE REPORT

PROJ. NO. [illegible] SPECIMEN NO. 9A CHG. NO. PSF-1 DATE 12/20/83

REQUESTED BY J. [illegible] MACHINE NO. 9

MATERIAL SPECIFICATION OR ALLOY

CONDITION

STRESS RUPTURE ✓ CREEP TEST

TEST TEMPERATURE 1800 STRESS 22.0KSI

OTHER INFORMATION OR REMARKS

DIAMETER .250 "

LOAD-PAN (20:1 BEAM 54.01 #

LOAD-SPECIMEN 1080.2 #

FINAL GAGE 1.191 "

ORIG. GAGE 1.000 "

DIFF. .191 "

ELONG. 19.1 %

DIAL GAGE-START

DIAL GAGE-STOP

DIFF.

ELONG. %

TIME OF DAY

INCREASE TO AT

INCREASE TO AT

INCREASE TO AT

INCREASE TO AT

TIMER READ.-FAIL OR STOP 21746.8

TIMER READING-START 21689.9

TEST TIME-HOURS 56.9

1/4/83

CREEP DATA:

FAILURE TYPE

NORMAL	✓
FAILED IN RADIUS	
FAILED OUTSIDE GAGE	
FAILED IN NOTCH	
FAILED IN THREADS	

FORM 2273

INDEX NO. 1611

CREEP – RUPTURE REPORT

PROJ. NO. PURDUE STUDENT SPECIMEN NO. 4B CHG. NO. P-5E-1 DATE 12/20/83

REQUESTED BY J. HECHT MACHINE NO. 7

MATERIAL SPECIFICATION OR ALLOY IN 738

CONDITION

STRESS RUPTURE ✓ CREEP TEST

TEST TEMPERATURE 1800 STRESS 22.0 KSI

OTHER INFORMATION OR REMARKS

DIAMETER .251 "

LOAD-PAN (20:1 BEAM 54.4 #

LOAD-SPECIMEN 1071.0 #

FINAL GAGE 1.085 "

ORIG. GAGE 1.000 "

DIFF. .085 "

ELONG. 8.5 %

DIAL GAGE-START

DIAL GAGE-STOP

DIFF.

ELONG. %

TIME OF DAY

INCREASE TO AT

INCREASE TO AT

INCREASE TO AT

INCREASE TO AT

TIMER READ.-FAIL OR STOP 0314.5

TIMER READING-START 0272.8

TEST TIME-HOURS 41.7

12/22/83

CREEP DATA:

FAILURE TYPE

NORMAL	
FAILED IN RADIUS	
FAILED OUTSIDE GAGE	✓
FAILED IN NOTCH	
FAILED IN THREADS	

1. Report No.	2. Government Accession No.	3. Recipient's Catalog No.
NASA CR-174762		

4. Title and Subtitle	5. Report Date
Effects of Cobalt, Boron, and Zirconium on the Microstructure of Udimet 738	September 1984
	6. Performing Organization Code
7. Author(s)	8. Performing Organization Report No.
Todd G. Nakanishi	None
	10. Work Unit No.
9. Performing Organization Name and Address	11. Contract or Grant No.
Purdue University West Lafayette, Indiana	NAG 3-59
	13. Type of Report and Period Covered
12. Sponsoring Agency Name and Address	Contractor Report
National Aeronautics and Space Administration Washington, D.C. 20546	14. Sponsoring Agency Code
	505-33-1A

15. Supplementary Notes

Final report. Project Manager, Coulson M. Scheuermann, Materials Division, NASA Lewis Research Center, Cleveland, Ohio 44135. This report was submitted as partial fulfillment of the requirements of the degree Master of Science in Engineering to Purdue University, West Lafayette, Indiana.

16. Abstract

A structural study was carried out on Co modified Udimet 738 alloys containing 0.04, 0.10, and 0.20 wt % Zr at 0.01 and 0.03 wt % B levels. Samples in the as-cast and solution-treated conditions were exposed at 843° C to study structural stability. The structures produced by the interactions of Co, Zr, and B were studied by SEM, X-ray diffraction and dispersive analysis techniques. The additions of large amounts of Zr and B were found to increase the solidification range of the U-738. Structural changes involved eutectic γ' islands, formation of low melting point compounds, and precipitation of borides and Zr rich phases. Boron and zirconium additions did not show substantial changes in mechanical properties. Removal of Co from the alloys resulted in reduction of the matrix solubility for carbon and increase in th γ' solvus. Structural instabilities found were continuous grain boundary $M_{23}C_6$ films, MC breakdown, and plate like phases. Removal of cobalt resulted in a slight decrease in tensile and stress rupture properties. Detailed structural results will be presented.

17. Key Words (Suggested by Author(s))	18. Distribution Statement
Nickel alloys; Microstructure; Heat resistant alloys; Cobalt; Boron; Metallography; Zirconium	Unclassified - unlimited STAR Category 26

19. Security Classif. (of this report)	20. Security Classif. (of this page)	21. No. of pages	22. Price*
Unclassified	Unclassified	75	A04

*For sale by the National Technical Information Service, Springfield, Virginia 22161

National Aeronautics and
Space Administration

Washington, D.C.
20546

Official Business
Penalty for Private Use, $300

SPECIAL FOURTH CLASS MAIL
BOOK

Postage and Fees Paid
National Aeronautics and
Space Administration
NASA-451

NASA

POSTMASTER: If Undeliverable (Section 158
Postal Manual) Do Not Return